Check for updates

Received: 24 November 2024 | Revised: 11 March 2025 | Accepted: 31 March 2025

DOI: 10.1002/suco.70090

ARTICLE

fib CEB-FIP WILEY

The workability, mechanical, and electrical properties of steel fiber-reinforced SCC incorporating ultra-fine copper slag as fine aggregate

Metin Katlav[1] | **Izzeddin Donmez**[2] | **Asim Kaygusuz**[3] | **Paki Turgut**[4] | **Kazim Turk**[4]

[1]Bitlis Eren University, Vocational School of Technical Sciences, Bitlis, Türkiye

[2]Adıyaman University, Vocational School of Technical Sciences, Adıyaman, Türkiye

[3]Inonu University, Engineering Faculty, Department of Electrical and Electronics Engineering, Malatya, Türkiye

[4]Inonu University, Engineering Faculty, Department of Civil Engineering, Malatya, Türkiye

Correspondence
Metin Katlav, Bitlis Eren University, Vocational School of Technical Sciences, Bitlis, Türkiye.
Email: mkatlav@beu.edu.tr

Funding information
Türkiye Bilimsel ve Teknolojik Araştırma Kurumu; Inönü Üniversitesi

Abstract

Ultra-fine copper slag (CS), a byproduct of the copper industry, is al waste material that is produced in large volumes annually, and its disposal and management are a major environmental concern. Therefore, the utilization of CS in various sectors, especially in the production of construction and building materials, offers enormous potential for both environmental sustainability and economic benefits. In this research, the feasibility of using CS at a ratio of 0%, 25%, 50%, 75%, and 100% by replacing fine aggregate in steel fiber-reinforced self-compacting concrete (SFR-SCC) with high-volume steel fiber (1.50% by volume) has been explored for the first time in the literature. To identify the workability properties of SFR-SCC mixes incorporating 0%, 25%, 50%, 75%, and 100% ultra-fine CS by replacing the fine aggregate, slump-flow, flow times (T500) and J-ring tests were performed, whereas compressive strength (f_c), splitting tensile strength (f_{ct}), and modulus of elasticity (E_c) tests were applied to the samples for different curing days to evaluate the mechanical properties. Additionally, electrical resistivity/conductivity tests were conducted to determine the electrical properties as well. The experimental results revealed that the inclusion of ultra-fine CS into SFR-SCC mixes with high-volume fiber improved the slump-flow and T500 values, whereas the use of ultra-fine CS above 50% induced a remarkable increase in the T500 value. In addition, the addition of ultra-fine CS caused significant decreases in *J*-ring height difference (ΔH) values, and a 4-times decrease in ΔH value was observed when the CS ratio was raised from 0% to 100%. In this context, in terms of workability, all mixes exhibited acceptable stability with minimal segregation tendency. On the other hand, the mechanical performance of SFR-SCC samples with

This is an open access article under the terms of the Creative Commons Attribution License, which permits use, distribution and reproduction in any medium, provided the original work is properly cited.
© 2025 The Author(s). *Structural Concrete* published by John Wiley & Sons Ltd on behalf of International Federation for Structural Concrete.

different ultra-fine CS ratios was found to be better than those without CS; specifically, the samples incorporating 25% ultra-fine CS reached outstanding values such as f_c, f_{ct}, and E_c with 83.4, 9.1, and 40.4 GPa, respectively. Furthermore, increasing the CS content in SFR-SCC samples led to considerable improvements in electrical properties, with the CS content raising the electrical conductivity values by an average of 60%. Consequently, it has been proven that the use of ultra-fine CS by replacing fine aggregate in SFR-SCC mixes having high-volume steel fiber improves both the workability and mechanical properties as well as its electrical performance, resulting in high-performance, eco-friendly composites. Thus, it also contributes to the protection of natural resources and the sustainable utilization of industrial waste as well as providing an innovative solution that improves the performance of building materials.

KEYWORDS

electrical properties, mechanical properties, steel fiber-reinforced SCC, ultra-fine copper slag, workability properties

1 | INTRODUCTION

Self-compacting concrete (SCC) is an innovative type of concrete developed by scholars in the late 1980s.[1] SCC is accepted as a high-performance concrete that can flow under its own weight without the need for vibration or compaction, fill mold cavities, and pass easily through high steel rebar density zones.[2–5] The primary objective in the production of this concrete is to minimize errors caused by the human factor in concreting and to reduce workmanship costs.[6] In addition, one of the most important benefits of SCC is that it offers much higher fluidity and stability compared to traditional concrete.[7–9] These characteristics widely favor SCC, particularly in the construction of complex and high steel rebar density structures, the covering of large areas, and the manufacture of prefabricated concrete elements.[10–12] The workability of SCC improves the uniformity of the concrete during the placing process in the molds, which ultimately leads to a higher compressive strength. Nevertheless, despite its high compressive strength, SCC's low tensile strength and toughness may cause unforeseen breaks in hardened states.[13–15] This can lead to unexpected damage, particularly in areas where tensile and flexural stresses are high. It can also negatively affect the durability of structures, shorten the service life, and potentially threaten structural integrity.[16,17] In order to address these problems, various types and ratios of fiber incorporation into SCC mixes have been proposed in many studies.[18–27] These studies[18–27] have shown that fiber addition significantly improves the mechanical and durability properties of SCC. In addition, the existence of fibers controls the post-cracking behavior of concrete, improving the energy absorption capacity of the composite and thus contributing to the maintenance of structural integrity by slowing down crack growth.[28–31] In particular, steel fibers are more favored for their potential to improve the load-carrying capacity, flexural tensile strength, toughness, and ductility of concrete as a consequence of their high bonding ability with concrete.[32–34] The random dispersion of steel fibers plays a vital role in enhancing the post-cracking behavior of steel fiber-reinforced (SFR)-SCC.[35,36] By controlling crack propagation at the micro level, steel fibers delay the formation of macro cracks, resulting in enhanced flexural rigidity.[19,37–39] Finally, the presence of steel fibers substantially improves the flexural behavior of reinforced concrete elements under different loads.[40–44] Nonetheless, even with all these collective benefits, there can be adverse effects on the permeability and productivity of SFR-SCC with a high content of steel fibers (over 1% by volume). The use of high amounts of steel fibers can make it difficult for the mix to reach the desired level of workability and may result in mechanical and other property criteria not being achieved to the anticipated degree.

On the other hand, SFR-SCC with a high steel fiber content necessitates the use of high amounts of cement to achieve the desired fresh and hardened concrete properties.[3,17] This can lead to both increased costs and an unsustainable composite.[45] In order to tackle this issue, the use of waste materials and by-products of various industries as aggregates and cement substitutes has

17517648, 0, Downloaded from https://onlinelibrary.wiley.com/doi/10.1002/suco.70090 by Metin Katlav - T C Inonu University . , Wiley Online Library on [10/04/2025]. See the Terms and Conditions (https://onlinelibrary.wiley.com/terms-and-conditions) on Wiley Online Library for rules of use; OA articles are governed by the applicable Creative Commons License

gained attention as a hopeful approach to achieving sustainable and eco-friendly composites as well as reducing production costs.[46–48] To achieve this, replacing cement or aggregate with supplementary cementitious materials (SCMs) in certain proportions in SFR-SCC can improve the mix's workability and mechanical properties, as well as significantly reducing the carbon footprint, energy consumption, and costs. The SCMs are generally preferred over industrial waste solids like blast furnace slag (BS), fly ash (FLA), silica fume, and copper slag (CS).[49–51] Especially in recent years, it has been emphasized that the use of CS as fine and coarse aggregate or cement substitute in concrete may have promising results in terms of achieving eco-friendly concrete with superior engineering properties.[52,53] During copper production, every 1000 kg of pure copper yields an average of 2500 kg of CS waste, which usually remains unutilized in the environment. Globally, each year generates nearly 70 million tons of CS waste.[53,54] However, storage of these wastes poses serious problems, such as negative environmental effects, high management costs, and the need for large storage areas.[55] Additionally, the quantity of natural resources that end up as industrial waste is growing annually. Considering from the viewpoint of a sustainable growth approach, the reuse of industrial by-products is the most cost-effective and reliable alternative. The building industry consumes more waste materials than other sector, making it the most appealing market for waste recycling. Notably, the annual production of concrete, which is the second most consumed material after water in the world, requires the use of large amounts of natural aggregates, with natural aggregates constituting about 65%–80% of the concrete volume.[56] This situation leads to rapid exhaustion of natural resources and serious damage to the environment. In order to minimize these negative effects and prevent irreparable damage to the environment, it is of great significance to use various industrial waste materials as aggregates in the concrete manufacturing process. Researchers highlight that CS can be utilized in the concrete sector in terms of its physical and chemical characteristics and that this material can not only solve waste management problems but also considerably mitigate environmental damages.[57–59] In this context, the unique workability, mechanical, and electrical properties of CS allow it to be used as a suitable fine aggregate in SFR-SCC mixes containing high volumes of steel fibers. The outstanding physical and chemical characteristics of CS enable it to be used as a replacement for fine aggregate, providing high performance concretes.[60,61] In the literature, there are many studies considering the use of CS as an aggregate replacement in traditional concrete[61–66] or non-fiber SCC[50,53,67–73]; according to the results of the studies, it has been demonstrated that the inclusion of CS in concrete considerably improved the workability, mechanical and durability properties. However, studies[74,75] examining the effects of CS on the workability and mechanical properties of SFR-SCC mixes are very limited. Moreover, only one study[76] has explored the electrical properties of SFR-SCC containing CS by replacing fine aggregate. Afshoon et al.[74] in their experimental study prepared SFR-SCC mixes incorporating 0.1%, 0.3%, and 0.5% by volume steel fiber and 20%, 30%, 40%, 50%, and 60% CS by replacing coarse aggregate and assessed their fresh and hardened characteristics. The results revealed that the use of CS dramatically improved the properties of SFR-SCC owing to its glassy texture and high density. Furthermore, the use of CS not only improved the flowability, passing ability, and fillability of the concrete, but also reduced the risk of segregation, despite increasing the steel fiber volume from 0.1% to 0.5%. Lastly, the use of 0.5% steel fiber by volume in the manufacture of SFR-SCC led to higher compressive strengths in all CS incorporated concrete compared to the control mix. These findings indicate that the combined use of CS and steel fibers is an effective approach to enhancing the mechanical performance of SFR-SCC. In another study, Katlav et al.[76] explored the electrical properties as well as the workability and mechanical properties of SFR-SCC incorporating 20%, 40%, 60%, and 80% BFS by replacing cement, 50% CS by replacing fine aggregate, and different hooked-end steel fiber lengths. According to the results of the mentioned work revealed that all SFR-SCC mixes exhibited satisfactory workability characteristics, and their compressive strength achieved an outstanding 127 MPa. The optimum amount of BS for higher compressive strength and conductivity was identified to be 40%. Additionally, the inclusion of CS significantly increased the electrical conductivity by around 363% and improved the compressive strength by nearly 9% compared to the mix without CS. The study's results demonstrate that waste materials from the iron and copper industries can prepare eco-friendly and sustainable electrically conductive cementitious composites, offering valuable insights for future electrically conductive concretes. However, more experimental research is required to fully assess the potential of CS in SFR-SCC, particularly in mixes with high-volume fiber. To the knowledge of the authors, there is no research examining the impact of using different proportions of ultra-fine CS replacing fine aggregate in SFR-SCC having high-volume fiber on workability, mechanical, and electrical properties. This highlights a significant knowledge gap in this field and provides a worthwhile area for researchers. Accordingly, in this paper, the influence of 0%, 25%, 50%, 75%, and 100% ultra-fine CS by replacing fine aggregate on

17517648, 0, Downloaded from https://onlinelibrary.wiley.com/doi/10.1002/suco.70090 by Metin Katlav - T C Inonu University . , Wiley Online Library on [10/04/2025]. See the Terms and Conditions (https://onlinelibrary.wiley.com/terms-and-conditions) on Wiley Online Library for rules of use; OA articles are governed by the applicable Creative Commons License

workability, mechanical, and electrical properties of SFR-SCC having 1.50% steel fiber volume was comprehensively examined.

1.1 | Research significance and motivation

The growth in the standard of living brought about by industrialization has nevertheless begun to cause serious and lasting problems for the environment. Production industries generate large amounts of waste and at the same time increase greenhouse gas emissions. This situation causes environmental pollution by uncontrolled mixing of wastes with soil, water, and air, resulting in adverse outcomes that endanger ecosystems and human health. Particularly, the storage and management of these wastes present significant environmental and economic challenges. On the other hand, the building industry consumes large amounts of natural resources for infrastructure projects, which causes rapid exhaustion of some natural resources and damage to the environment. The intensive consumption of raw materials such as natural aggregates and cement used in concrete production causes irreversible damage to natural ecosystems. In this context, the primary motivation of this research is the use of ultra-fine CS, waste of the copper industry, as a fine aggregate substitute in SFR-SCC mixes having high-volume steel fiber. The utilization of CS not only solves waste management problems but also contributes to the development of more sustainable, cost-effective, and eco-friendly concrete composites in the building industry. In addition, for the first time, the effects of using ultra-fine CS by replacing the fine aggregate at different ratios in SFR-SCC mixes on the workability, mechanical, and electrical properties are investigated, thus revealing the potential use of this waste material in the production of high-performance concrete. Such an approach both decreases the environmental footprint and enables the development of more cost-effective construction materials from an economic point of view.

2 | EXPERIMENTAL METHODS

2.1 | Properties of raw ingredients

The main ingredients used to manufacture SFR-SCC mixes are generally: Portland pozzolan cement (PPC) CEM IV 32.5R with low CO_2 emissions, *F* class FLA, BS, CS, aggregates, water, high-range water reducer admixture (HWRA), and steel fiber. Table 1 presents the chemical and physical characteristics of PPC, FLA, BS, and CS, while Figure 1 displays the microstructural characteristics of these materials obtained by scanning electron microscopy.

As for the aggregates used in SFR-SCC mixes, fine and coarse aggregates with water absorption values of 1.80% and 0.80%, respectively, were selected. The specific gravities of these aggregates were determined as 2.43 and

TABLE 1 The chemical composition and physical properties of PPC, FLA, BS, and CS.

Composition	PPC	FLA	BS	CS
Chemicals	(%)			
CaO	45.6	1.07	32.92	5.35
SiO_2	30.1	63.09	32.37	34.28
Al_2O_3	7.5	21.63	10.00	3.47
Fe_2O_3	3.9	6.77	1.33	49.21
MgO	2.3	-	9.77	0.9
SO_3	2.5	0.10	0.70	-
K_2O	0.9	-	0.83	-
Na_2O	0.9	2.79	0.42	-
CuO	-	-	-	0.51
Other	6.30	4.55	11.66	6.28
$SiO_2 + Al_2O_3 + Fe_2O_3$	41.50	91.49	43.7	86.96
LOI	3.45	2.68	-	-
Physical properties				
Specific gravity	2.97	2.30	2.86	3.66
Specific surface area (cm^2/g)	4370	2900	4085	-

17517648, 0, Downloaded from https://onlinelibrary.wiley.com/doi/10.1002/suco.70090 by Metin Katlav - T C Inonu University . , Wiley Online Library on [10/04/2025]. See the Terms and Conditions (https://onlinelibrary.wiley.com/terms-and-conditions) on Wiley Online Library for rules of use; OA articles are governed by the applicable Creative Commons License

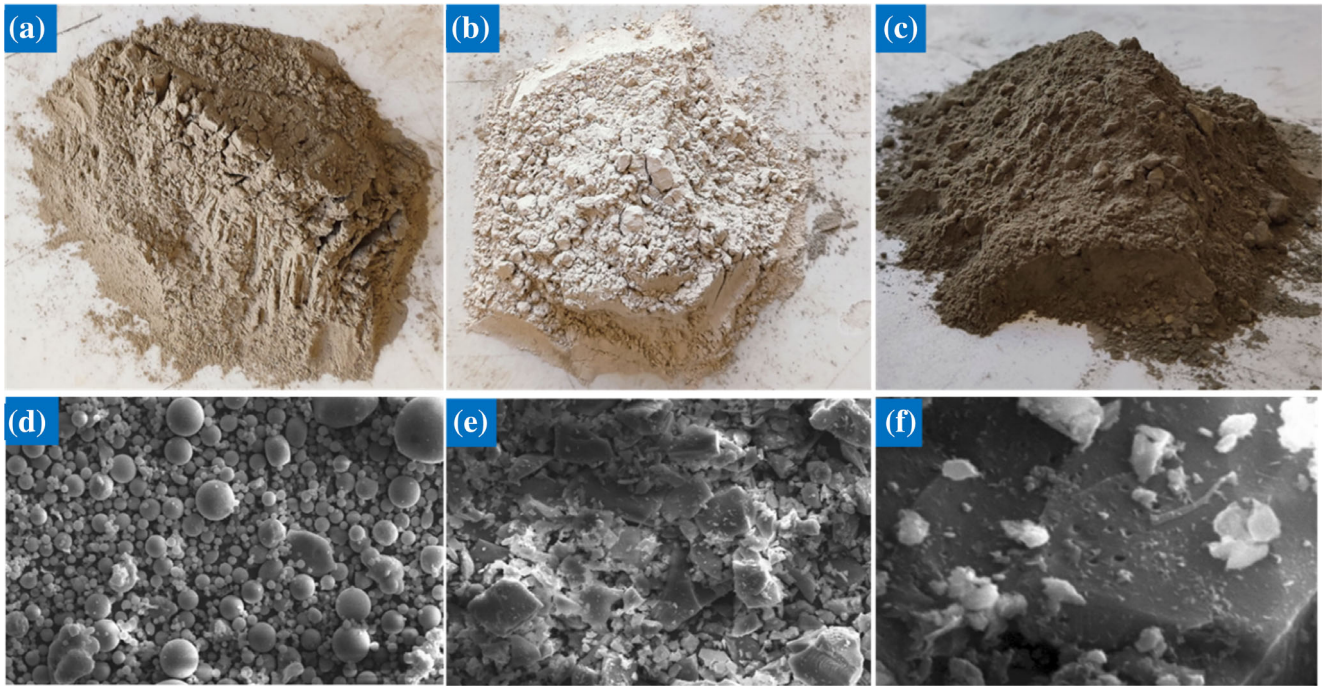


FIGURE 1 Macrostructure of (a) FLA, (b) BS, (c) CS; microstructure of (d) FLA, (e) BS, (f) CS.

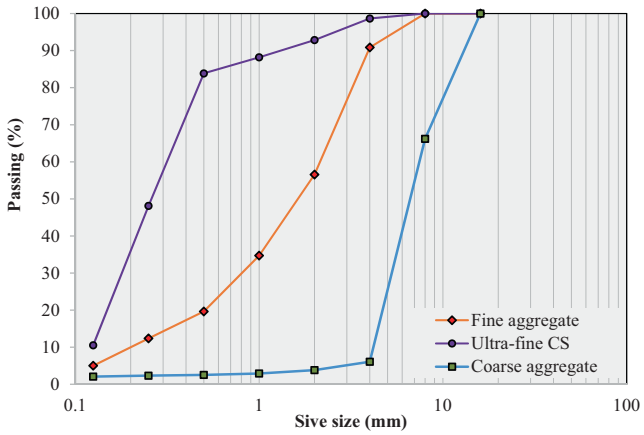


FIGURE 2 Distribution of the particle size of aggregates.

2.69, respectively. The findings of the sieve analysis for coarse and fine aggregates are presented in Figure 2.

Moreover, Figure 2 presents the sieve analysis results of CS, which is to be used in the replacement of fine aggregate. Meanwhile, it is worth noting that the ultra-fine CS has a water absorption value of 7.80% due to its void and ultra-fine structure (see Figures 1f and 2). Meanwhile, the CS was used in its as-sourced form without any grinding or additional processing, at no extra cost or energy expenditure. This approach allowed the slag to be directly utilized in concrete mixes, supporting both economic and environmental sustainability. Lastly, HWRA based on polycarboxylic polymer with a density of 1.05 g/cm^3 and a pH value of 5–7 was integrated into mixes to enhance the fresh properties of SFR-SCC.

In addition to all these, in the scope of the work, in the manufacture of SFR-SCC mixes, a hooked-end steel fiber having a length of 35 mm and a diameter of 0.75 mm was chosen, as shown in Figure 3. The tensile strength and modulus of elasticity of this steel fiber were determined as 1250 and 200 GPa, respectively.

2.2 | Mix proportions and preparation

In this work, mix designs were scrupulously conducted to identify the effects of using different ratios of ultra-fine CS by replacing the fine aggregate on the workability, mechanical, and electrical properties of SFR-SCC. To this end, the SF3 slump flow class (760–850 mm) proposed according to EFNARC (2005)[77] was considered for developing SFR-SCC mixes, with optimal mix proportions identified through a trial-and-error procedure. In the SFR-SCC mixes, ultra-fine CS by replacing the fine aggregate was used in five different ratios of 0%, 25%, 50%, 75%, and 100%. In addition, in order to evaluate the effect of using a high volume of ultra-fine CS on SFR-SCC mixes, the hooked-end steel fiber ratio was constant in all mixes at 1.50% by volume. To minimize the adverse impact of the high volume of steel fibers on the workability of SFR-SCC mixes, for all mixes the amount of binder material (PPC + FLA + BS) was kept constant at

17517648, 0, Downloaded from https://onlinelibrary.wiley.com/doi/10.1002/suco.70090 by Metin Katlav - T C Inonu University . , Wiley Online Library on [10/04/2025]. See the Terms and Conditions (https://onlinelibrary.wiley.com/terms-and-conditions) on Wiley Online Library for rules of use; OA articles are governed by the applicable Creative Commons License

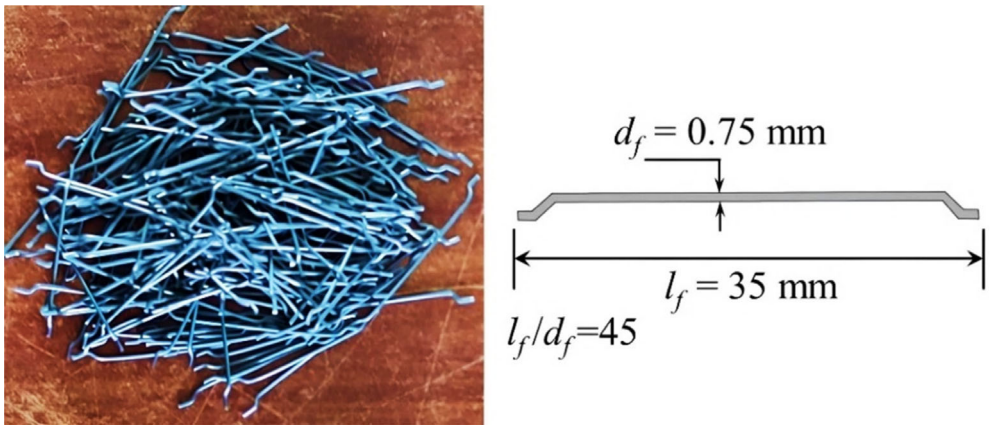


FIGURE 3 Geometrical shape of fiber used in the research.

TABLE 2 The amounts of ingredients of SFR-SCC (kg/m^3).

	Binder			Aggregate						
Mix name	**PPC**	**FLA**	**BS**	**Fine**	**Coarse**	**CS**	**CS substitution ratio**	**Water**	**Steel fiber**	**HWRA**
CS0	400	250	350	624	155	-	0	300	117.75	4.50
CS0.25	400	250	350	491	164	164	%25	300	117.75	10.25
CS0.50	400	250	350	351	175	351	%50	300	117.75	15.25
CS0.75	400	250	350	188	188	565	%75	300	117.75	16.50
CS1.00	400	250	350	-	200	800	%100	300	117.75	28.00

1000 kg/m^3, whereas the fine aggregate to total aggregate ratio was selected as 80%. Meanwhile, it is worth pointing out that the amount of HWRA was determined by trial-and-error for each mix to achieve the targeted slump flow class. Ultimately, the ingredients amount of prepared SFR-SCC mixes based on the dry state of all the aggregates is detailed in Table 2.

A concrete mixer with a total capacity of 35 dm^3 was used to manufacture the SFR-SCC mixes incorporating 0%, 25%, 50%, 75%, and 100% of ultra-fine CS by replacing the fine aggregate. The following steps were followed during the preparation of the mixes: (i) At the beginning, all aggregates (fine and coarse, as well as CS, if available), hooked-end steel fibers, and two thirds of the mix water were included in the mixer and mixed for 3.5 min until a homogeneous mix was obtained. (ii) Then, the binder materials (PPC, FLA, and BS) were added to the mixer. (iii) Finally, HWRA and the remaining mix water were added, and the mix was mixed for another 6.5 min. Eventually, SFR-SCC mixes were attained with a total mixing time of 10 min (refer to Figure 4).

2.3 | Experiments methods

Slump flow, flow times (T500), and *J*-ring tests were conducted to assess the workability properties of SFR-SCC mixes incorporating 0%, 25%, 50%, 75%, and 100% of ultra-fine CS by replacing the fine aggregate, while compressive strength, splitting tensile strength, and modulus of elasticity tests were applied to identify the mechanical properties. Moreover, electrical resistivity tests were performed to determine the electrical performance of SFR-SCC as well. Thus, together with these tests, they aim to comprehensively evaluate the performance of the concrete mixes in both fresh and hardened states. Meanwhile, the use of high volumes of ultra-fine CS in SFR-SCC mixes may extend the hydration process. In this context, all samples were kept in the molds for 48 h. This was done to maintain the integrity of the samples due to early demolding.

2.4 | Workability performance experiments

A slump-flow and T500 test was undertaken to measure the flowability and viscosity characteristics of SFR-SCC mixes incorporating 0%, 25%, 50%, 75%, and 100% of ultra-fine CS by replacing the fine aggregate (see Figure 5a). In this test, a standard slump cone was used, and the concrete was poured freely into the cone without compacting. After filling the slump cone with the SFR-SCC mix, two vertical diameters were measured as the

17517648, 0, Downloaded from https://onlinelibrary.wiley.com/doi/10.1002/suco.70090 by Metin Katlav - T C Inonu University , , Wiley Online Library on [10/04/2025]. See the Terms and Conditions (https://onlinelibrary.wiley.com/terms-and-conditions) on Wiley Online Library for rules of use; OA articles are governed by the applicable Creative Commons License



FIGURE 4 The procedure for preparing SFR-SCC mixes.

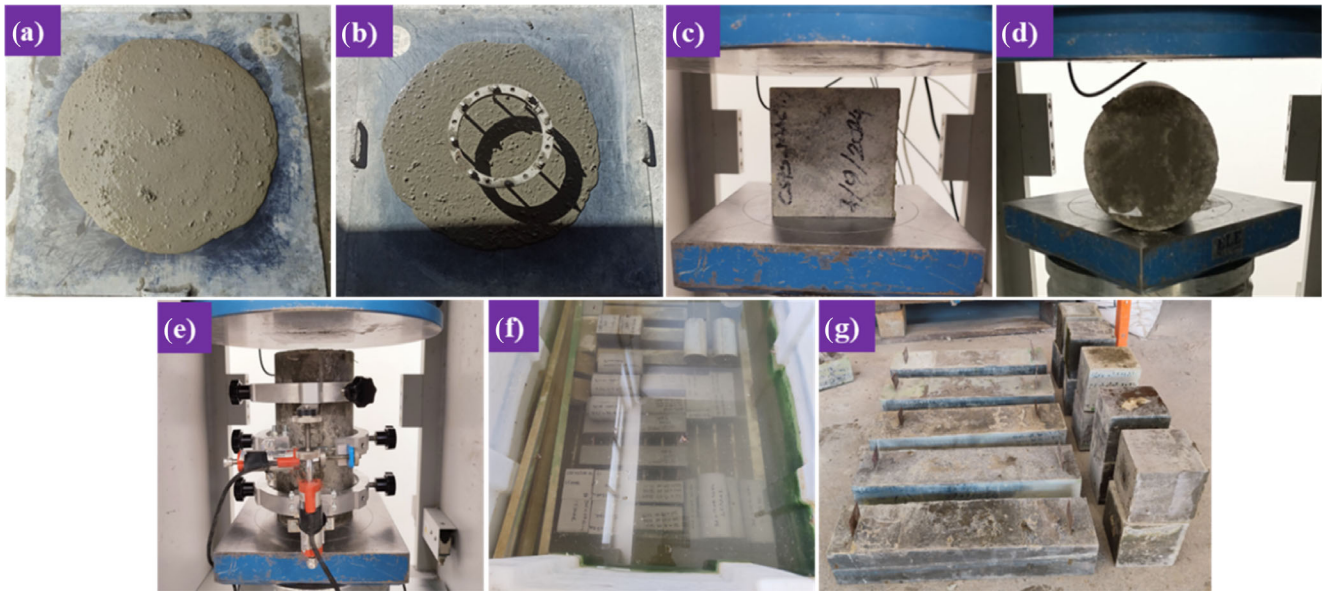


FIGURE 5 Workability and mechanical testing of mixes, along with sample preparation and curing conditions.

sample spread under its own weight, and the slump-flow diameter was determined by averaging these values. Meanwhile, the flow times taken for the slump-flow diameter to reach 500 mm (T500) were also recorded. Additionally, the *J*-ring test was applied to evaluate the passability of SFR-SCC mixes incorporating 0%, 25%, 50%, 75%, and 100% of ultra-fine CS by replacing the fine aggregate. In this test, the *J*-ring apparatus was mounted on a circle with a diameter of 300 mm, and a slump cone was inserted into it, and the steps of the slump-flow test

17517648, 0, Downloaded from https://onlinelibrary.wiley.com/doi/10.1002/suco.70090 by Metin Katlav - T C Inonu University , , Wiley Online Library on [10/04/2025]. See the Terms and Conditions (https://onlinelibrary.wiley.com/terms-and-conditions) on Wiley Online Library for rules of use; OA articles are governed by the applicable Creative Commons License

were followed (refer to Figure 5b). The *J*-ring height difference ($H_2-H_1=\Delta H$) of the SFR-SCC mixes was then calculated by the average of the height differences measured at four different points between the inside and that just outside. Meanwhile, it is important to note that all workability tests were conducted in compliance with the specifications and limit values proposed by the EFNARC.[77,78]

2.4.1 | Mechanical performance experiments

The samples were prepared to identify the compressive strength (f_c), splitting tensile strength (f_{ct}), and elastic modulus (E_c) of SFR-SCC mixes incorporating 0%, 25%, 50%, 75%, and 100% of ultra-fine CS by replacing the fine aggregate. Three 100 × 100 × 100 mm cubic samples for compressive strength, three φ100 × 200 mm cylindrical samples for splitting tensile strength, and two φ100 × 200 mm cylindrical samples for elastic modulus testing were used. The compressive and splitting tensile strength tests were conducted after the samples were cured for 7, 28, and 56 days, whereas the elastic modulus tests were performed only after 56 days of curing. Meanwhile, it is important to highlight that all samples were kept at a relative humidity of 100% and a temperature of 23 ± 2°C throughout the work. The compressive strength test was done with a 3000 kN press device applying axial load at 6 kN/s according to BS 12390-3[79] (see Figure 5c), while a load rate during the tests of splitting tensile strength and elastic modulus was applied as 1.60 and 1.80 kN/s, respectively, in accordance with ASTM C496[80] and ASTM C469[81] (refer to Figure 5d, e). Lastly, via the stress–strain curve from the elastic modulus test, the ASTM C469[81] elastic modulus value was calculated (Equation (1)).

$$E_c=\frac{0.4\times f_c-f_1}{\varepsilon_2-0.00005}, \tag{1}$$

where f_c is the ultimate compressive strength, f_1 is the stress corresponding to a longitudinal strain of 50×10^{-6} and ε_2 is the longitudinal strain produced by stress at 40% of f_c.

2.4.2 | Electrical conductivity experiment

In order to measure the electrical conductivity of SFR-SCC mixes incorporating 0, 25, 50, 75, and 100% of ultra-fine CS by replacing the fine aggregate, two prism samples with the size of 100 mm × 75 mm × 400 mm were fabricated for each mix. Stainless copper electrode meshes of 60 mm × 60 mm were used to achieve a uniform current flow in the samples (refer to Figure 6a). The electrodes were inserted into the cross-section of the samples, positioned 35 mm apart from each edge. All samples were cured under water at 23 ± 2°C until the test days (see Figure 5f). To assure the consistency of the electrical conductivity tests and to overcome the effect of surface moisture, the samples were tested in the dry condition and at an ambient temperature of 25°C for curing periods of 28 and 56 days (Figure 5g). This research employed a straightforward and dependable two-probe testing procedure, which has shown efficacy in several investigations.[82–85] Figure 6 depicts a schematic representation of the two-probe testing setup. This technique involves the application of a potential difference between two meshes that are placed into the sample. The resulting electric current (Amper) between the two electrodes is then measured in response to the applied voltage. Subsequently, electrical resistivity values were calculated according to Equation (2). Besides, it is worth emphasizing that a uniform potential difference of 30 V was applied to every SFR-SCC sample incorporating 0%, 25%, 50%, 75%, and 100% of ultra-fine CS by replacing the fine aggregate.

$$\rho=\frac{U\times A_c}{L_e\times I}, \tag{2}$$

where ρ represents resistivity (Ω.cm), U indicates voltage (V), A_c means cross-sectional area of the concrete sample (cm^2), L_e symbolizes distance between electrodes (cm), and I represents electric current (A).

3 | THE EXPERIMENTAL RESULTS AND DISCUSSION

3.1 | Workability properties

3.1.1 | Slump-flow and T500 test results

Figure 7 illustrates the slump-flow and T500 values of SFR-SCC mixes incorporating 0%, 25%, 50%, 75%, and 100% of ultra-fine CS by replacing the fine aggregate. By referring to Figure 7, it is concluded that the slump-flow values of all the mixes manufactured vary between 760 and 795 mm, demonstrating that all SFR-SCC mixes are classified as SF3 based on EFNARC. The CS1.00 mix, which contains 100% CS by replacing the fine aggregate, had the highest slump-flow value with 795 mm, while the CS0 mix, which does not contain CS, had the lowest value with 760 mm. Nevertheless, it should be highlighted that the T500 values vary in the range of 6–

17517648, 0, Downloaded from https://onlinelibrary.wiley.com/doi/10.1002/suco.70090 by Metin Katlav - T C Inonu University , , Wiley Online Library on [10/04/2025]. See the Terms and Conditions (https://onlinelibrary.wiley.com/terms-and-conditions) on Wiley Online Library for rules of use; OA articles are governed by the applicable Creative Commons License

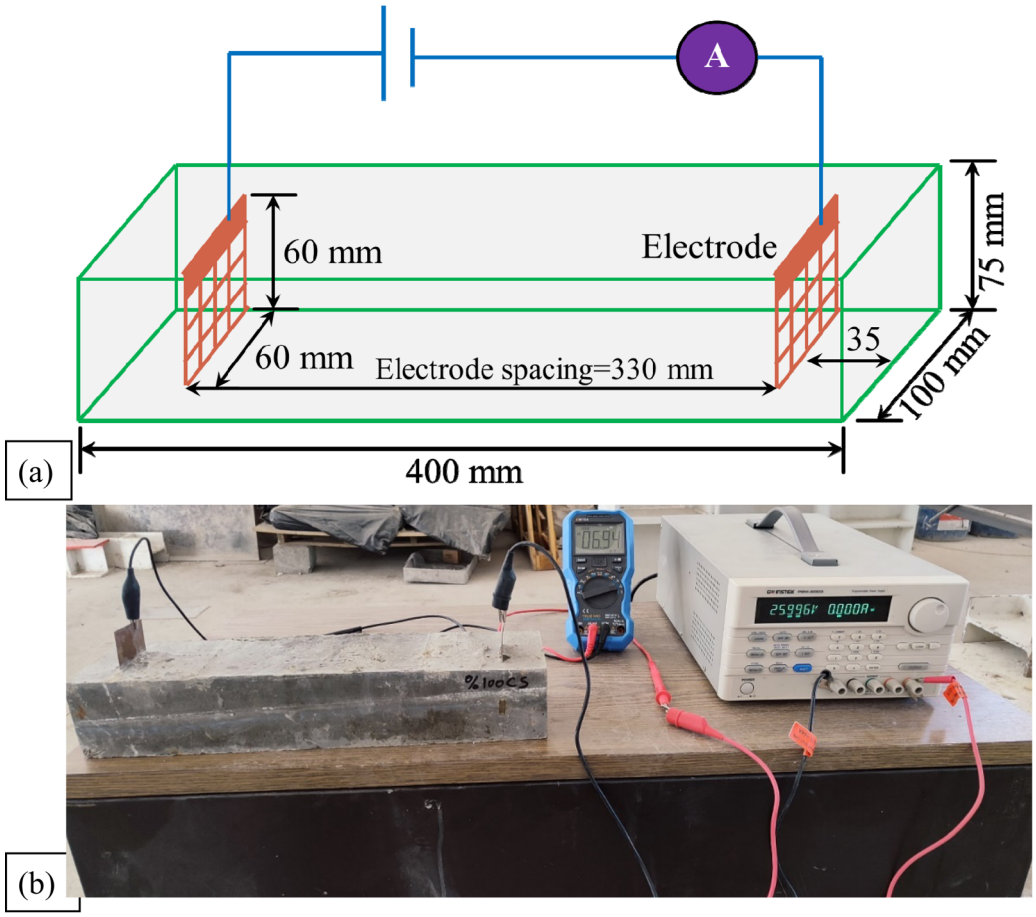


FIGURE 6 Electrical conductivity test setup.

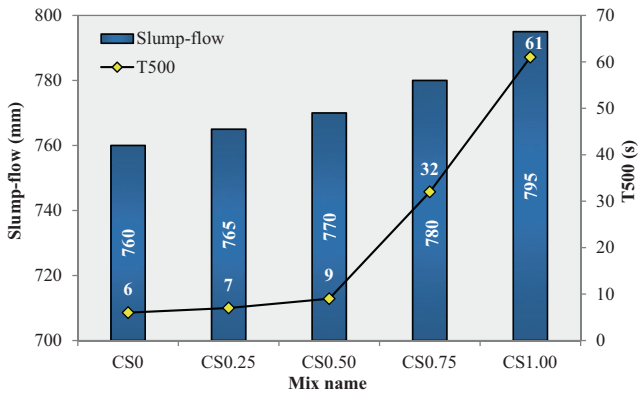


FIGURE 7 Slump-flow and T500 values of SFR-SCC mixes incorporating different ratios of ultra-fine CS.

61 s, and these results are outside the limit values (2–5 s) suggested by EFNARC.[77,78] Meanwhile, it should be remembered that the workability limit values suggested by EFNARC are defined for SCC without fiber.[77,78]

Referring to Figure 7, the slump-flow and T500 values of the mixes increase as the CS ratio increases. Nonetheless, due to its water absorption capacity of 7.80%, a higher amount of HWRA was needed to achieve satisfactory workability. In particular, the use of more than 50% CS by replacing the fine aggregate caused a significant increment in the T500 values. For instance, the T500 value of the CS0 mix without CS was 6 s, whereas the CS1.00 mix containing 100% CS reached 61 s, that is, approximately 10 times higher (refer to Figure 7). This may be ascribed to the dense structure and smooth glassy surface of ultra-fine CS, which improve the viscosity of the mixes. Several studies[8,50,53,69,70,74] in the literature have proven that CS, by replacing the fine aggregate in different ratios, considerably improves SCC's workability in terms of stability. However, previous studies[8,50,53,69,70,74] used CSs with a lower water absorption capacity, which led to a reduction in the need for superplasticizer to achieve the required flowability. From this point of view, the high-water absorption capacity of the ultra-fine CS used in this research necessitates the use of more superplasticizer, which suggests the need to consider the effects of this material on workability in a different aspect in future studies.

The visual stability index (VSI), as defined in the ASTM C1611[86] standard, was used to assess the stability

17517648, 0, Downloaded from https://onlinelibrary.wiley.com/doi/10.1002/suco.70090 by Metin Katlav - T C Inonu University - , Wiley Online Library on [10/04/2025]. See the Terms and Conditions (https://onlinelibrary.wiley.com/terms-and-conditions) on Wiley Online Library for rules of use; OA articles are governed by the applicable Creative Commons License

of SFR-SCC mixes incorporating 0%, 25%, 50%, 75%, and 100% of ultra-fine CS by replacing the fine aggregate. The VSI is based on some characteristics that are visually inspected to determine the segregation tendency of SCC mixes. As per the ASTM C1611, VSI values are classified as 0, 1, 2, and 3. These values define the stability of the SCC mix as follows:

- VSI = 0: The mix is highly stable, with no signs of segregation or bleeding.
- VSI = 1: The mix is considered stable; there is no segregation, but there may be a small amount of bleeding.
- VSI = 2: The mix is considered unstable; some aggregate segregation is observed in the middle of the mix.
- VSI = 3: The mix is considered highly unstable, with large aggregate segregation occurring in the middle of the mix.

The VSI values of SFR-SCC mixes incorporating 0%, 25%, 50%, 75%, and 100% of ultra-fine CS by replacing the fine aggregate are depicted in Figure 8. By examining Figure 8, the VSI values of CS0.25 and CS1.00 mixes containing 25% and 100% ultra-fine CS were 0, indicating that these mixes were highly stable and did not exhibit any evidence of segregation or bleeding. Conversely, the VSI values of CS0, CS0.50, and CS0.75 mixes containing 0%, 50%, and 75% CS were found to be 1.50 (see Figure 8c and d), pointing to a very slight segregation tendency of these mixes. These findings indicate that despite the high amount of steel fiber (by volume 1.50%) and CS contained in the mixes, all the mixes had satisfactory stability, and the segregation propensity remained at a minimal level. To conclude, it can be emphasized that ultra-fine CS contributes positively to the stability of SFR-SCC mixes generally. This can be attributed to the homogeneous distribution of ultra-fine CS in the mix and its strong cohesive effect between the aggregates.[87]

3.1.2 | *J*-ring test results

Figure 9 reports the *J*-ring flow and ΔH values of SFR-SCC mixes incorporating 0%, 25%, 50%, 75%, and 100% of ultra-fine CS by replacing the fine aggregate. Considering Figure 9, it is seen that the ΔH values vary between 4 and 16 mm, and the ΔH values of all mixes except for the CS0 mix without CS are below the 10 mm limit specified according to EFNARC.[77,78] Meanwhile, it is

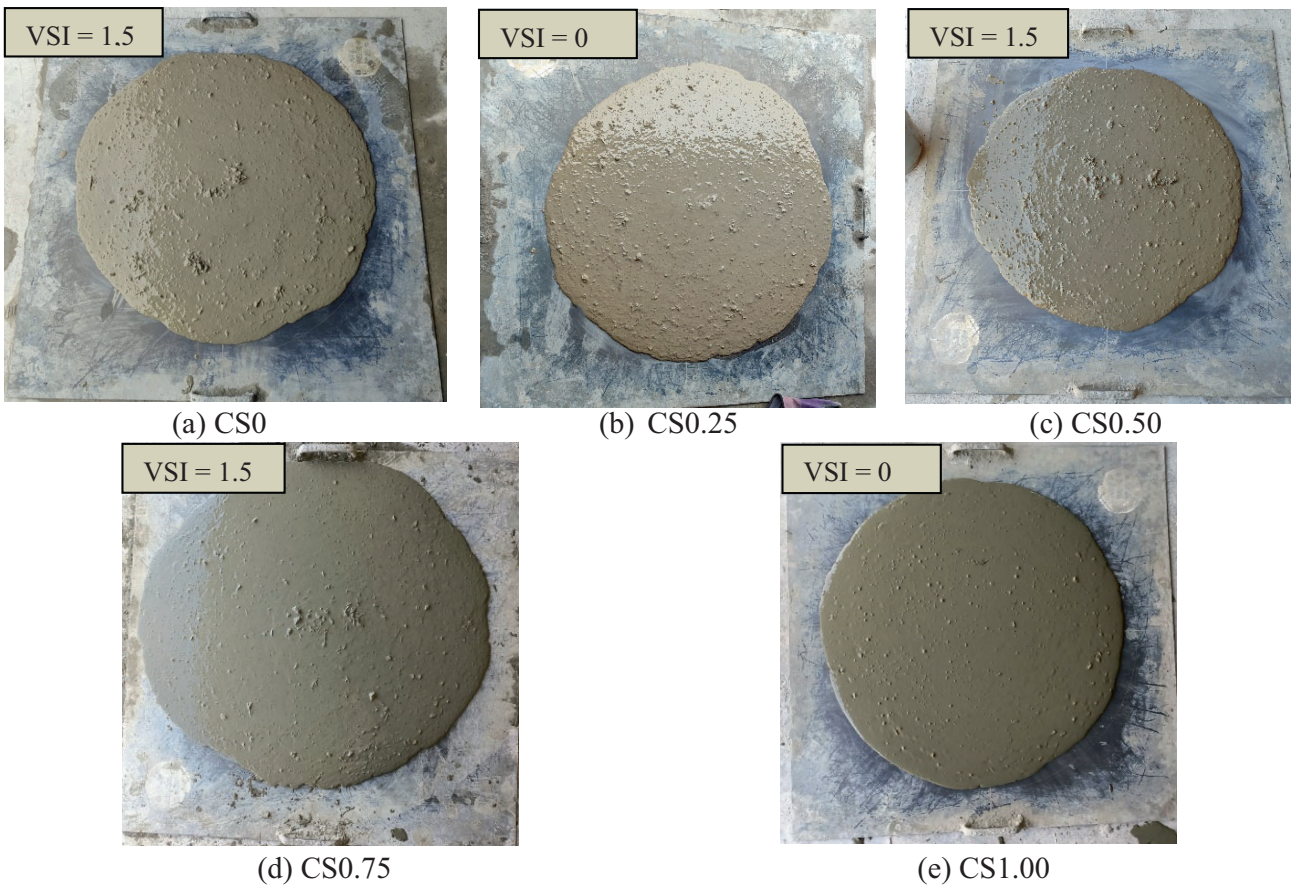


FIGURE 8 VSI values of SFR-SCC mixes incorporating different ratios of ultra-fine CS.

17517648, 0, Downloaded from https://onlinelibrary.wiley.com/doi/10.1002/suco.70090 by Metin Katlav - T C Inonu University . , Wiley Online Library on [10/04/2025]. See the Terms and Conditions (https://onlinelibrary.wiley.com/terms-and-conditions) on Wiley Online Library for rules of use; OA articles are governed by the applicable Creative Commons License

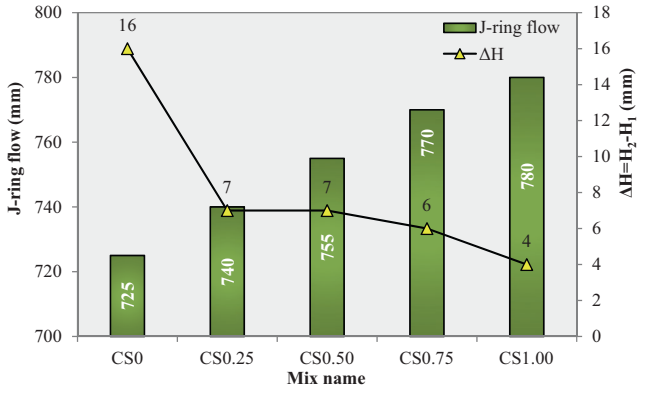


FIGURE 9 *J*-ring flow and Δ*H* values of SFR-SCC mixes incorporating different ratios of ultra-fine CS.

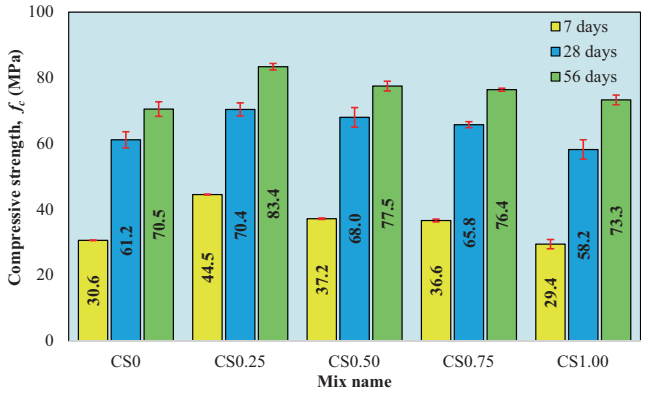


FIGURE 10 7-, 28-, and 56-days f_c values of SFR-SCC mixes incorporating different ratios of ultra-fine CS. (a) CS0, (b) CS0.25, (c) CS0.50, (d) CS0.75, (e) CS1.00.

important to note that EFNARC's suggestions are for SCC mixes without fiber. Additionally, the *J*-ring flow values showed a variation in the range of 725–780 mm. This implies that the addition of ultra-fine CS can improve the passing ability of SFR-SCC mixes.

Specifically, the highest *J*-ring flow and lowest Δ*H* values were achieved in the CS1.00 mix containing 100% CS with 780 and 4 mm, respectively (see Figure 9). In contrast, the CS0 mix without CS achieved the lowest *J*-ring flow and the highest Δ*H* values, measuring 725 and 16 mm, respectively. These findings demonstrate that there is an increase in *J*-ring flow and a decreasing tendency in Δ*H* values with increasing CS content. The reasons for these results can be attributed to several factors: (i) The smooth and glassy surface of the ultra-fine CS increases fluidity because it reduces friction between the mix's other ingredients and the CS particles; (ii) The high-water absorption capacity of the ultra-fine CS absorbs some of the water in the mix, improving viscosity and thus reducing the risk of segregation, ultimately leading to a decrease in Δ*H* values.

Consequently, it can be inferred that increasing the ultra-fine CS content in SFR-SCC mixes, despite its high fiber volume (1.50%), enhances the flowability and passing ability of the mixes and thus may contribute to the achievement of the desired mechanical and electrical properties. Notwithstanding, replacing fine aggregate with ultra-fine CS at a ratio of more than 50% may probably have a negative effect on the workability of SFR-SCC mixes because the T500 time significantly increased. This result indicates that replacing fine aggregate with ultra-fine CS in SFR-SCC mixes should not exceed 50%. Additionally, more comprehensive research is needed to determine the optimum amount of ultra-fine CS in SFR-SCC mixes. Such studies are critical for better understanding the effects of ultra-fine CS on workability and mechanical performance in SFR-SCC mixes, as well as determining the optimum ratios for electrical properties.

3.2 | Mechanical properties

3.2.1 | Compressive strength

Figure 10 displays the 7-, 28-, and 56-days f_c values of SFR-SCC samples incorporating 0%, 25%, 50%, 75%, and 100% ultra-fine CS by replacing the fine aggregate, along with the error bars. Referring to Figure 10, the 7-days f_c of the samples is between 29 and 45 MPa, the 28-days f_c ranges from 58 to 71 MPa, and the 56-days f_c is varied within the range of 70 to 84 MPa. These findings indicate that, taking into account the ultimate strength, all samples can be categorized as high-strength concrete based on ACI 363R-10.[88]

Looking at Figure 10, the highest f_c values for 7, 28, and 56 days were achieved in CS0.25 samples containing 25% CS with 44.5, 70.4, and 83.4 MPa, respectively. By contrast, the lowest f_c value for 7 and 28 days was observed in CS1.00 samples containing 100% CS with 29.4 and 58.2 MPa, respectively, whereas the lowest f_c value for 56 days was found in CS0 samples without CS with 70.5 MPa. On the other hand, as can be seen from Figure 10, the incorporation of CS by replacing fine aggregate in SFR-SCC samples resulted in generally higher f_c at all curing times. In other words, the incorporation of CS increased the f_c of SFR-SCC samples by approximately 1.20, 1.07, and 1.10 times at 7, 28, and 56 days of curing, respectively, indicating a significant improvement compared to the samples without CS. The f_c enhancement of ultra-fine CS in SFR-SCC samples can be attributed to three main reasons as mentioned in a review work[89]: (i) the high density, abrasiveness, and

17517648, 0, Downloaded from https://onlinelibrary.wiley.com/doi/10.1002/suco.70090 by Metin Katlav - T C Inonu University , , Wiley Online Library on [10/04/2025]. See the Terms and Conditions (https://onlinelibrary.wiley.com/terms-and-conditions) on Wiley Online Library for rules of use; OA articles are governed by the applicable Creative Commons License

compactability of CS particles may enhance the strength by enabling the release of concentrated stresses within the concrete[61,90]; (ii) the smooth surface and sharp edges of CS may improve the bond strength of the concrete matrix, leading to a reinforced structure[63,91,92]; (iii) because of its small particle size, CS may fill voids in the mix and act as filler, thereby increasing the strength of concrete.[93] Various studies[76,94–96] in the literature have reported findings that support the results of the present study. For instance, in the study of Katlav et al.,[76] it was reported that when 50% CS was used by replacing fine aggregate in hybrid fiber-reinforced SCC, f_c increased by nearly 9%. Likewise, in another study,[94] it was stated that SCC mixes incorporating up to 30% CS as fine aggregate resulted in an 11% increment in f_c value compared to SCC mixes without CS. Furthermore, Chaitanya and Sivakumar[95] in their study observed a 40% improvement in f_c at the end of the 28-days curing period when they replaced 20% of the fine aggregate with CS in SCC. Lastly, Ameri et al.[96] verified that enhancing the fine CS aggregates up to 60% in concretes incorporating 0.10% steel fiber improves the f_c by 12% compared to the control mix.

In addition to all these, in order to more clearly demonstrate the influence of CS on the f_c of SFR-SCC samples, the cement intensity index (CII) was calculated and is reported in Figure 11. This index is based on the procedure recommended by Damineli et al.[97] and indicates the amount of cement needed in 1 m^3 of concrete to achieve a f_c of 1 MPa. In this work, CII values were calculated based on the 56-days f_c values of the samples, taking into account the effects due to pozzolanic reactions of binder materials.

Considering Figure 11, CII values of SFR-SCC samples incorporating 0%, 25%, 50%, 75%, and 100% ultra-fine CS by replacing the fine aggregate ranged from 4.80 to 5.70 $kg.m^{-3}.MPa^{-1}$. The CS0.25 samples incorporating 25% CS with the highest f_c (83.4 MPa) had the lowest CII of 4.80 $kg.m^{-3}.MPa^{-1}$, while the CS0 mix without CS with the lowest f_c (70.50 MPa) had the highest CII of 5.70 $kg.m^{-3}.MPa^{-1}$. These findings highlight that the use of CS is critical for achieving eco-friendly and sustainable high-strength SFR-SCC. To summarize, all mixes incorporating CS have lower CII values compared to mixes without CS, implying that less cement is required to achieve unit strength, thereby promoting sustainability.

3.2.2 | Splitting tensile strength

The 7-, 28-, and 56-days f_{ct} results of SFR-SCC samples incorporating 0%, 25%, 50%, 75%, and 100% ultra-fine CS by replacing the fine aggregate are summarized in Figure 12 by taking the average of the three samples tested. According to Figure 12, the 7-, 28-, and 56-days f_{ct} values of the samples vary between 3.0–4.5 MPa, 7.1–7.7 MPa, and 8.4–9.1 MPa, respectively.

Regarding Figure 12, it is noted that the highest values of f_{ct} for all curing ages were achieved in CS0.25 samples containing 25% CS; the f_{ct} values of these samples were 4.5 MPa for 7 days, 7.7 MPa for 28 days, and 9.1 MPa for 56 days. Nevertheless, the lowest f_{ct} values in general for all curing ages were observed in CS1.00 samples containing 100% CS; the f_{ct} values for 7, 28, and 56 days were found to be 3.0, 7.1, and 8.4 MPa, respectively. Additionally, Figure 12 shows that using up to 75% CS usually improved the f_{ct} values of SFR-SCC samples for all curing ages compared to samples without CS, but it is evident that using 100% CS by replacing the fine aggregate generally lowers these f_{ct} values. These results are quite compatible with previous studies in the literature.[69,98] For example, Siddique et al.[98] reported that the use of different proportions of CS replacing the fine aggregate in traditional fiber concrete incorporating 1% steel fiber by volume enhanced the 56-days f_{ct} values by

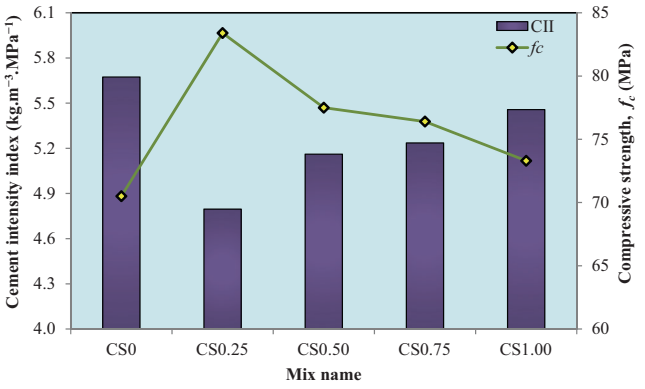


FIGURE 11 CII value of the SFR-SCC mixes for 56 days.

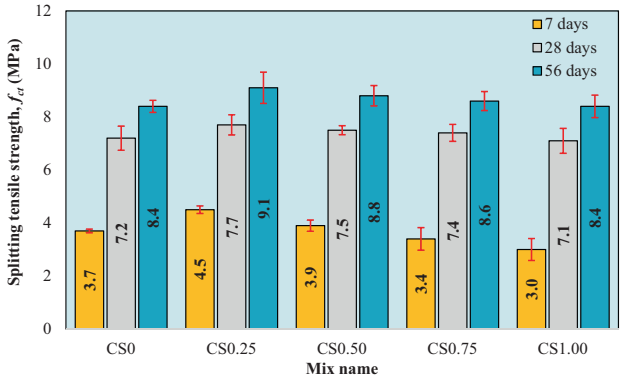


FIGURE 12 7-, 28-, and 56-days f_{ct} values of SFR-SCC mixes incorporating different ratios of ultra-fine CS.

17517648, 0, Downloaded from https://onlinelibrary.wiley.com/doi/10.1002/suco.70090 by Metin Katlav - T C Inonu University . , Wiley Online Library on [10/04/2025]. See the Terms and Conditions (https://onlinelibrary.wiley.com/terms-and-conditions) on Wiley Online Library for rules of use; OA articles are governed by the applicable Creative Commons License

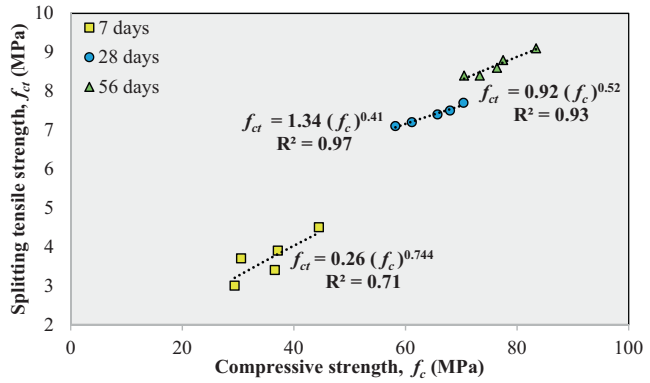


FIGURE 13 Relationship between f_c and f_{ct} of SFR-SCC mixes incorporating different ratios of ultra-fine CS.

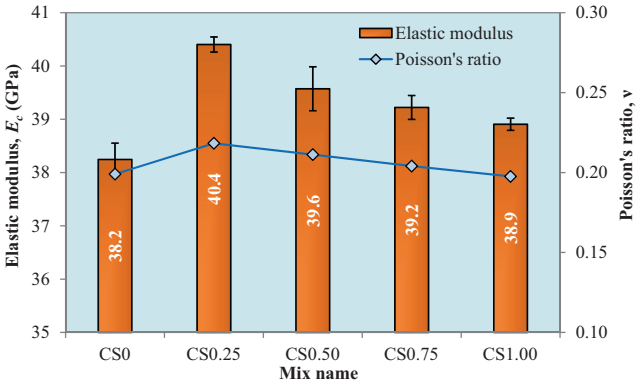


FIGURE 14 The E_c and ν values of the SFR-SCC samples for 56 days.

approximately 1.24 times in comparison to the samples without CS. The researchers explained that at high CS volumes, the particle packing effect plays a crucial role in enhancing concrete's tensile strength. Likewise, in another study by Sharifi et al.,[69] it was noted that the f_{ct} of concrete incorporating CS in the range of 10%–100% improved by nearly 4%–48%.

In addition to all these, regression analysis was undertaken to examine the relationship between f_c and f_{ct} of SFR-SCC samples incorporating 0%, 25%, 50%, 75%, and 100% ultra-fine CS by replacing the fine aggregate for each curing day. At the end of these analyses, the presence of an exponential relationship between f_c and f_{ct} values in the form of $y = ax^n$ was revealed (see Figure 13). As illustrated in Figure 13, the R^2 values achieved for 7-, 28-, and 56-days samples are 0.71, 0.97, and 0.93, respectively, representing that the proposed equations have high accuracy and can be used practically by design engineers. Meanwhile, the calculated R^2 values for all equations are above 0.70, which verifies that these equations have admissible accuracy because statistical theory dictates that a prediction equation must have an R^2 value of at least 0.70 to be considered reliable.[99–102]

3.2.3 | Elastic modulus

The modulus of elasticity, a parameter associated with material rigidity, signifies the ability of cementitious composites to undergo elastic deformation. In context, Figure 14 illustrates the 56-days modulus of elasticity (E_c) and Poisson's ratio (ν) values of SFR-SCC samples incorporating 0%, 25%, 50%, 75%, and 100% ultra-fine CS by replacing the fine aggregate designed within the scope of the present study. It is worth noting that the values in Figure 14 are the average of the two samples tested. As can be seen in Figure 14, the E_c values ranged from 38.2 to 40.4 GPa, and the ν values were 0.21 on average. The highest E_c was recorded in CS0.25 samples containing 25% CS with 40.2 GPa. Conversely, the CS0 samples without CS recorded the lowest E_c at 38.2 GPa. These results imply that using ultra-fine CS in SFR-SCC mixes leads to improvements in the E_c. The inclusion of ultra-fine CS in the concrete mix may have achieved a particle packing effect, resulting in a denser and more homogeneous structure of the concrete matrix.[50]

In addition to all these, regression analysis was undertaken to identify the relationship between f_c and E_c for SFR-SCC samples incorporating 0%, 25%, 50%, 75%, and 100% ultra-fine CS by replacing the fine aggregate. Besides, the relationship between the experimentally obtained E_c and the predicted E_{pred} values using the equation (Equation (3)) proposed by ACI 318[19][103] was examined. As shown in Figure 15a, the relationship between f_c and E_c of the produced concretes is linear and has a very high accuracy with $R^2 = 0.99$. This demonstrates that the proposed equation for SFR-SCC samples incorporating ultra-fine CS is practically applicable. On the other hand, when Figure 15b is considered, it is evident that there is a strong correlation ($R^2 = 0.99$) between E_c obtained from experiments and predicted E_{pred}. This points out that E_c can be predicted with high accuracy when f_c values of SFR-SCC samples are available.

$$E_c = 4700\sqrt{f_c} \quad \text{(ACI 318 – 19)}. \tag{3}$$

3.3 | Electrical properties

Figure 16 displays the electrical resistivity and conductivity values of SFR-SCC samples incorporating 0%, 25%, 50%, 75%, and 100% ultra-fine CS replacing the fine

17517648, 0, Downloaded from https://onlinelibrary.wiley.com/doi/10.1002/suco.70090 by Metin Katlav - T C Inonu University . , Wiley Online Library on [10/04/2025]. See the Terms and Conditions (https://onlinelibrary.wiley.com/terms-and-conditions) on Wiley Online Library for rules of use; OA articles are governed by the applicable Creative Commons License

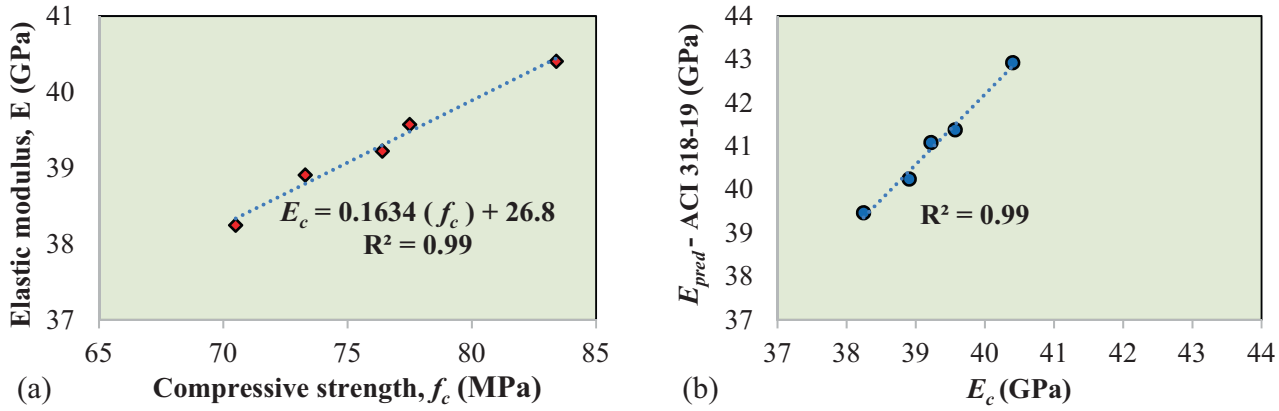


FIGURE 15 The correlation between; (a) f_c and E_c, (b) E_c and ACI 318-19 prediction model.

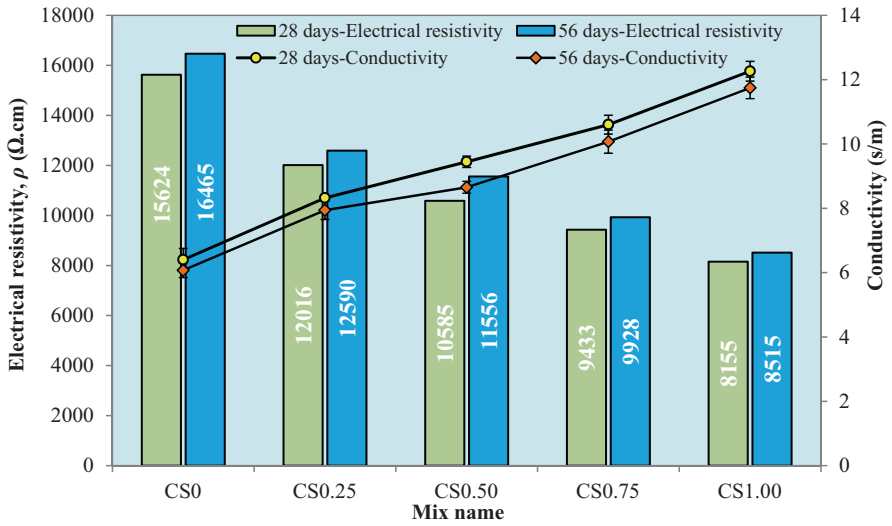


FIGURE 16 28- and 56-days electrical resistivity and conductivity values of SFR-SCC mixes incorporating different ratios of ultra-fine CS.

aggregate for 28 and 56 days; these values represent the average of the two samples tested. When Figure 16 is examined, it is observed that the electrical resistivity values of the SFR-SCC samples are between 8155 and 15624 Ω.cm for 28 days and the conductivity values are in the range of 6.4–12.3 s/m. As for the 56-day samples, electrical resistivity ranged within the range of 8515–16465 Ω.cm and conductivity ranged between 6.1 and 11.7 s/m. Meanwhile, a slight increase in electrical resistivity and a decrease in conductivity were observed as the curing time increased. This can be related to the decrease in moisture contributing to the conductivity of the concrete as a result of hydration reactions as the age of the concrete increases.[104]

Considering Figure 16, among the SFR-SCC samples containing ultra-fine CS, the lowest electrical resistivity and highest conductivity values for both 28- and 56-days curing times were obtained from CS1.00 samples containing 100% CS. For these samples, electrical resistivity values were determined as 8155 Ω.cm for 28 days and 8515 Ω.cm for 56 days; conductivity values were recorded as 12.3 and 11.7 s/m, respectively. On the contrary, the highest electrical resistivity and lowest conductivity values were measured in CS0 samples without CS; 28-days electrical resistivity and conductivity values were 15624 Ω.cm and 6.4 s/m, while 56-days values were 16465 Ω.cm and 6.1 s/m, respectively. On the other hand, as can be seen in Figure 16, there is a dramatic decrease in the electrical resistivity values of SFR-SCC samples as the CS content increases. For instance, for 28-days curing time, when the CS content was increased from 0% to 25%, 50%, 75%, and 100%, the electrical resistivity values reduced by 1.30, 1.48, 1.66, and 1.92 times, while for 56-days curing time, these values were measured as 1.31, 1.42, 1.66, and 1.93 times, respectively. This clearly reveals that ultra-fine CS has a considerable effect on the electrical characteristics of concrete, and the electrical resistivity shows a substantial decrease with high-volume CS content. This may be attributed to the composition of ultra-fine CS containing copper oxide (CuO) and

17517648, 0, Downloaded from https://onlinelibrary.wiley.com/doi/10.1002/suco.70090 by Metin Katlav - T C Inonu University , , Wiley Online Library on [10/04/2025]. See the Terms and Conditions (https://onlinelibrary.wiley.com/terms-and-conditions) on Wiley Online Library for rules of use; OA articles are governed by the applicable Creative Commons License

high content of iron oxide (Fe_2O_3) (see Table 1). In other words, given that CuO and Fe_2O_3 have a certain conductivity, they are thought to provide the connection between the steel fibers within the concrete, promoting the formation of conductive pathways and thus contributing to the decrease of electrical resistivity. Various studies[76,105] in the literature have proved that CS substantially improves the electrical conductivity values of concrete. In the meantime, the electrical properties of SFR-SCC mixes containing ultra-fine CS derived in this work showed better performance in comparison with existing studies[106,107] that used the same amount of steel fiber. For instance, in one work,[106] the electrical properties and heating performance of hybrid SFR SCC having 1.00%, 1.25%, and 1.50% by volume were examined. The findings showed that samples with 1.50% fiber by volume had the lowest electrical resistivity (17,350 Ω.cm) and the highest f_c (78 MPa). Moreover, Fiala et al.[107] found that SFR concretes with varying fiber volumes (0%, 0.5%, 1.0%, and 2.0%) had electrical resistivity values of 31000 Ω.cm for 1% steel fiber and 35000 Ω.cm for 2% steel fiber by volume. Although these investigations have different mixing ratios, the resistivity values obtained from this work are substantially superior to those in previous research.

Lastly, regression analysis was applied between CS ratios and the normalized electrical resistivity ($\rho/\sqrt{f_c}$) values for each curing day; it should be mentioned that the $\rho/\sqrt{f_c}$ value has been proposed in prior works.[76,106] As a result of the analysis, it was observed that there is a parabolic relationship between CS ratios and $\rho/\sqrt{f_c}$ values in the form of $y = ax^2 + bx + c$ (see Figure 17). Conclusively, the parabolic relationship between CS ratios and $\rho/\sqrt{f_c}$ values was found to be high precision ($R^2 = 0.97$ for 28 days and $R^2 = 0.94$ for 56 days samples). Additionally, the mathematical equations derived for electrical resistivity estimation of SFR-SCC samples for each curing day are provided in Equations (4) and (5). From this point of view, it can be emphasized that these equations can be used as an effective and robust tool to estimate the electrical resistivity of SFR-SCC samples containing different proportions of ultra-fine CS.

$$\rho_{28-\text{days}} = \left(1109.9(\text{CS})^2 - 1960.6(\text{CS}) + 1953\right) \times \sqrt{f_c} \Rightarrow R^2 = 0.97, \tag{4}$$

$$\rho_{56-\text{days}} = \left(881.4(\text{CS})^2 - 1751.7(\text{CS}) + 1902\right) \times \sqrt{f_c} \Rightarrow R^2 = 0.94 \tag{5}$$

4 | CONCLUSION AND FUTURE PERSPECTIVES

This research investigates the impact of different ratios of ultra-fine CS by replacing fine aggregate on the workability, mechanical, and electrical properties of SFR-SCC mixes with 1.50% hooked-end steel fiber by volume. Some of the important conclusions that emerged based on the results and discussions are as follows:

- In SFR-SCC mixes with high-volume fiber, the addition of ultra-fine CS by replacing the fine aggregate increased the slump-flow and T500 values of the mixes. Especially, it is remarkable that the addition of more than 50% CS by replacing the fine aggregate caused a significant increase in the T500 value. To conclude, it can be emphasized that the mixes exhibited satisfactory stability with minimal segregation tendency despite the high amount of steel fiber.
- The inclusion of ultra-fine CS by replacing the fine aggregate in SFR-SCC mixes resulted in remarkable

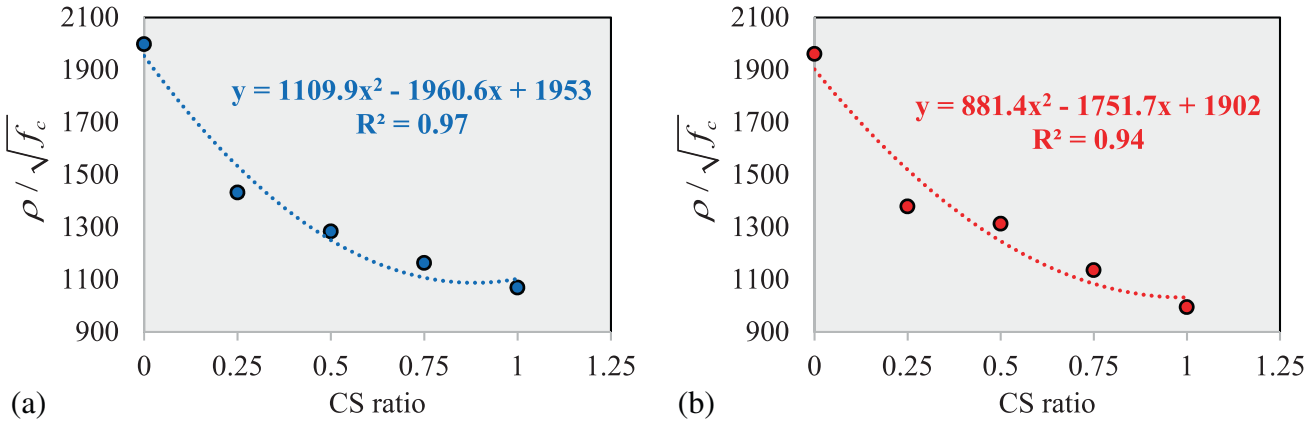


FIGURE 17 Relationship between CS ratios and $\rho/\sqrt{f_c}$ values; (a) 28 days (b) 56 days.

17517648, 0, Downloaded from https://onlinelibrary.wiley.com/doi/10.1002/suco.70090 by Metin Katlav - T C Inonu University , , Wiley Online Library on [10/04/2025]. See the Terms and Conditions (https://onlinelibrary.wiley.com/terms-and-conditions) on Wiley Online Library for rules of use; OA articles are governed by the applicable Creative Commons License

decreases in ΔH values. For instance, increasing the amount of CS from 0% to 100% reduced the ΔH value by 4 times, implying that ultra-fine CS is a precious alternative to improve the passing ability of SFR-SCC mixes with high-volume steel fiber.

- The samples incorporating different ratios of ultra-fine CS exhibited better mechanical performance compared to the samples without CS. Specifically, samples CS0.25 containing 25% ultra-fine CS replacing the fine aggregate demonstrated the best mechanical performance at all curing ages. When considering the ultimate strength at 56 days, the CS0.25 samples achieved exceptional f_c, f_{ct}, and E_c values of 83.4 MPa, 9.1 MPa, and 40.4 GPa, respectively.
- Increasing the amount of ultra-fine CS in SFR-SCC samples led to a remarkable improvement in electrical properties, and high CS content resulted in significant decreases in electrical resistivity values. For all curing days, the inclusion of CS decreased the electrical resistivity values by about 1.60 times on average compared to the samples without CS. These results demonstrated the effectiveness of CS as an alternative material to enhance conductivity in electrically conductive concrete applications. The use of CS as a substitute for fine aggregate will not only enhance the electrical conductivity of concrete but will also contribute significantly to the conservation of natural resources and economic design options.

As a conclusion, the SFR-SCC incorporating ultra-fine CS developed in this paper can be considered as an important alternative innovative concrete in the production of large span structures, dams, tunnels, precast concrete elements, and conductive concrete due to its high workability, mechanical, and electrical properties. However, this research utilized only one type of steel fiber with hooked-end and a single fiber volume of 1.50%. This necessitates a more thorough investigation into the performance of various fiber volumes and combinations in SFR-SCC mixes containing ultra-fine CS. Furthermore, the use of ultra-fine CS as a cement replacement is an area that has not been sufficiently studied in the literature and potentially remains to be explored. Lastly, it is of great importance to investigate the durability properties of SFR-SCC incorporating ultra-fine CS in detail so that it can be used reliably in the construction industry.

AUTHOR CONTRIBUTIONS

Metin Katlav: Writing—review and editing, writing—original draft, visualization, validation, methodology, investigation, formal analysis, conceptualization. **Izzeddin Donmez**: Writing-original draft, validation, methodology, investigation, conceptualization. **Asim Kaygusuz**: Investigation, methodology, writing—review and editing. **Paki Turgut**: Investigation, methodology,writing—review and editing. **Kazim Turk**: Writing—review and editing, investigation, validation, methodology, conceptualization.

ACKNOWLEDGMENTS

This study was supported by the Scientific and Technological Research Council of Turkiye (TUBITAK) under Grant Number 123 M595 and the Scientific Research Projects Committee of Inonu University under Grant Number FDK-2024-3507. The authors thank both institutions for their financial support.

DATA AVAILABILITY STATEMENT

The data that support the findings of this study are available from the corresponding author upon reasonable request.

ORCID

Metin Katlav https://orcid.org/0000-0001-9093-7195
Izzeddin Donmez https://orcid.org/0000-0002-2721-4215
Asim Kaygusuz https://orcid.org/0000-0003-2905-1816
Paki Turgut https://orcid.org/0000-0002-3711-4605
Kazim Turk https://orcid.org/0000-0002-6314-9465

REFERENCES

1. Okamura H, Ouchi M. Sel-compacting concrete. J Adv Concrete Technol. 2003;5–15.
2. Bayat H, Banar R, Nikravan M, Farnood P, Ramezanianpour AM, Kashani A. Durability, mechanical, workability, and environmental assessment of self-consolidating concrete containing blast furnace slag and natural zeolite. J Build Eng. 2024;86:108737. https://doi.org/10.1016/j.jobe.2024.108737
3. Katlav M, Turk K, Turgut P. Flexural performance of *V*-shaped RC folded plates: The role of plate thickness and fiber hybridization. Construct Build Mater. 2023;400:132815. https://doi.org/10.1016/j.conbuildmat.2023.132815
4. Katlav M. The effect of different fiber combination on the thickness of *V*-shaped reinforced concrete folded plate elements produced with steel fiber reinforced SCC, M.Sc. Dissertation, Institute of Science, Inonu University. 2022. https://doi.org/10.13140/RG.2.2.35968.51207
5. Hasan-Nattaj F, Nematzadeh M. The effect of forta-ferro and steel fibers on mechanical properties of high-strength concrete with and without silica fume and nano-silica. Construct Build Mater. 2017;137:557–72. https://doi.org/10.1016/j.conbuildmat.2017.01.078
6. Nehdi M, Pardhan M, Koshowski S. Durability of self-consolidating concrete incorporating high-volume replacement composite cements. Cem Concr Res. 2004;34:2103–12. https://doi.org/10.1016/j.cemconres.2004.03.018
7. Ahmad J, Zhou Z. Mechanical performance of waste marble based self compacting concrete reinforced with steel fiber

17517648, 0, Downloaded from https://onlinelibrary.wiley.com/doi/10.1002/suco.70090 by Metin Katlav - T C Inonu University . , Wiley Online Library on [10/04/2025]. See the Terms and Conditions (https://onlinelibrary.wiley.com/terms-and-conditions) on Wiley Online Library for rules of use; OA articles are governed by the applicable Creative Commons License

(part I). J Build Eng. 2023;78:107574. https://doi.org/10.1016/j.jobe.2023.107574
8. Sharma R, Khan RA. Fresh and mechanical properties of self compacting concrete containing copper slag as fine aggregates. J Mater Eng. 4.1 (2017):25–36.
9. García Calvo JL, Alonso MC, Fernández Luco L, Robles Velasco M. Durability performance of sustainable self compacting concretes in precast products due to heat curing. Construct Build Mater. 2016;111:379–85. https://doi.org/10.1016/j.conbuildmat.2016.02.097
10. Cui T, Kulasegaram S, Li H. Design automation of sustainable self-compacting concrete containing fly ash via data driven performance prediction. J Build Eng. 2024;87:108960. https://doi.org/10.1016/j.jobe.2024.108960
11. Turk K, Katlav M, Turgut P. Investigation of workability and engineering properties of hybrid fiber reinforced SCC mixtures. Bitlis Eren Univ J Sci. 2022;11:400–10 [in Turkish]. https://doi.org/10.17798/bitlisfen.984473
12. Turk K, Katlav M, Bitkin RE. The use of high-volume hybrid steel fiber instead of compression rebar to improve the structural performance of high-strength SCC beams under bending. Construct Build Mater. 2025;470:140521. https://doi.org/10.1016/j.conbuildmat.2025.140521
13. Aslani F, Liu Y, Wang Y. The effect of NiTi shape memory alloy, polypropylene and steel fibres on the fresh and mechanical properties of self-compacting concrete. Construct Build Mater. 2019;215:644–59. https://doi.org/10.1016/j.conbuildmat.2019.04.207
14. Thakare AA, Singh A, Gupta V, Siddique S, Chaudhary S. Sustainable development of self-compacting cementitious mixes using waste originated fibers: a review. Resour Conserv Recycl. 2021;168:105250. https://doi.org/10.1016/j.resconrec.2020.105250
15. Ergen F, Katlav M. Investigation of optimized machine learning models with PSO for forecasting the shear capacity of steel fiber-reinforced SCC beams with/out stirrups. J Build Eng. 2024;83:108455. https://doi.org/10.1016/j.jobe.2024.108455
16. Da Silva PR, De Brito J. Experimental study of the porosity and microstructure of self-compacting concrete (SCC) with binary and ternary mixes of fly ash and limestone filler. Construct Build Mater. 2015;86:101–12. https://doi.org/10.1016/j.conbuildmat.2015.03.110
17. Donmez I, Katlav M, Turk K. Improvement of fresh and hardened properties of a sustainable HFRSCC using various powders as multi-blended binders. Construct Build Mater. 2023;371:130773. https://doi.org/10.1016/j.conbuildmat.2023.130773
18. Khaloo A, Raisi EM, Hosseini P, Tahsiri H. Mechanical performance of self-compacting concrete reinforced with steel fibers. Construct Build Mater. 2014;51:179–86. https://doi.org/10.1016/j.conbuildmat.2013.10.054
19. Katlav M, Turk K, Turgut P. The impact of different length hooked-end fibers on the structural performance of RC folded plates. Struct Concr. 2024;26(1):179–96. https://doi.org/10.1002/suco.202301064
20. Gueciouer D, Youcef G, Tarek N. Rheological and mechanical optimization of a steel fiber reinforced self-compacting concrete using the design of experiments method. Eur J Environ Civ Eng. 2019;26(3):1097–117. https://doi.org/10.1080/19648189.2019.1697758
21. Wang W, Shen A, Lyu Z, He Z, Nguyen KTQ. Fresh and rheological characteristics of fiber reinforced concrete—a review. Construct Build Mater. 2021;296:123734. https://doi.org/10.1016/j.conbuildmat.2021.123734
22. Ghasemi M, Ghasemi MR, Mousavi SR. Studying the fracture parameters and size effect of steel fiber-reinforced self-compacting concrete. Construct Build Mater. 2019;201:447–60. https://doi.org/10.1016/j.conbuildmat.2018.12.172
23. Katlav M, Turk K, Turgut P. Research into effect of hybrid steel fibers on the V-shaped RC folded plate thickness. Structure. 2022;44:665–79. https://doi.org/10.1016/j.istruc.2022.08.046
24. Hasan R, Sobuz MHR, Akid ASM, Awall MR, Houda M, Saha A, et al. Eco-friendly self-consolidating concrete production with reinforcing jute fiber. J Build Eng. 2023;63:105519. https://doi.org/10.1016/j.jobe.2022.105519
25. Haddadou N, Chaid R, Ghernouti Y, Adjou N. The effect of hybrid steel fiber on the properties of fresh and hardened self-compacting concrete. J Build Mater Struct. 2014;1(2):65–76. https://doi.org/10.34118/jbms.v1i2.10
26. Pająk M, Ponikiewski T. Flexural behavior of self-compacting concrete reinforced with different types of steel fibers. Construct Build Mater. 2013;47:397–408. https://doi.org/10.1016/j.conbuildmat.2013.05.072
27. Turk K, Oztekin E, Kina C. Self-compacting concrete with blended short and long fibres: experimental investigation on the role of fibre blend proportion. Eur J Environ Civ Eng. 2019;26(3):905–18. https://doi.org/10.1080/19648189.2019.1686069
28. Teng S, Afroughsabet V, Ostertag CP. Flexural behavior and durability properties of high performance hybrid-fiber-reinforced concrete. Construct Build Mater. 2018;182:504–15. https://doi.org/10.1016/j.conbuildmat.2018.06.158
29. Yoo DY, Yoon YS. Structural performance of ultra-high-performance concrete beams with different steel fibers. Eng Struct. 2015;102:409–23. https://doi.org/10.1016/j.engstruct.2015.08.029
30. Yoo DY, Moon DY. Effect of steel fibers on the flexural behavior of RC beams with very low reinforcement ratios. Construct Build Mater. 2018;188:237–54. https://doi.org/10.1016/j.conbuildmat.2018.08.099
31. Turk K, Katlav M, Turgut P. Effect of rebar arrangements on the structural behavior of RC folded plates manufactured from hybrid steel fiber-reinforced SCC. J Build Eng. 2024;84:108680. https://doi.org/10.1016/j.jobe.2024.108680
32. Zhao C, Wang Z, Zhu Z, Guo Q, Wu X, Zhao R. Research on different types of fiber reinforced concrete in recent years: an overview. Construct Build Mater. 2023;365:130075. https://doi.org/10.1016/j.conbuildmat.2022.130075
33. Alshahrani A, Kulasegaram S. Effect of fibre diameter and tensile strength on the mechanical, fracture, and fibre distribution properties of eco-friendly high-strength self-compacting concrete. Construct Build Mater. 2023;403:133161. https://doi.org/10.1016/j.conbuildmat.2023.133161
34. Zhang P, Wang C, Guo J, Wu J, Zhang C. Production of sustainable steel fiber-reinforced rubberized concrete with enhanced mechanical properties: a state-of-the-art review. J Build Eng. 2024;91:109735. https://doi.org/10.1016/j.jobe.2024.109735
35. Li N, Jin Z, Long G, Chen L, Fu Q, Yu Y, et al. Impact resistance of steel fiber-reinforced self-compacting concrete (SCC)

17517648, 0, Downloaded from https://onlinelibrary.wiley.com/doi/10.1002/suco.70090 by Metin Katlav - T C Inonu University , , Wiley Online Library on [10/04/2025]. See the Terms and Conditions (https://onlinelibrary.wiley.com/terms-and-conditions) on Wiley Online Library for rules of use; OA articles are governed by the applicable Creative Commons License

at high strain rates. J Build Eng. 2021;38:102212. https://doi.org/10.1016/j.jobe.2021.102212
36. Kesavamoorthi R, Mohan Ganesh G. Impact resistance of micro and macro crimped steel fibre reinforced self-compacting concrete with SCM. Case Stud Constr Mater. 2023;19:e02452. https://doi.org/10.1016/j.cscm.2023.e02452
37. Kim GW, Choi H-J, Piao R, Oh T, Koh K, Lim K, et al. Influence of hybrid reinforcement effects of fiber types on the mechanical properties of ultra-high-performance concrete. Construct Build Mater. 2024;426:135995. https://doi.org/10.1016/j.conbuildmat.2024.135995
38. Di Carlo F, Spagnuolo S. Cracking behavior of steel fiber-reinforced concrete members subjected to pure tension. Struct Concr. 2019;20:2069–80. https://doi.org/10.1002/suco.201900048
39. Yoo DY, Yang JM. Effects of stirrup, steel fiber, and beam size on shear behavior of high-strength concrete beams. Cem. Concr Compos. 2018;87:137–48. https://doi.org/10.1016/j.cemconcomp.2017.12.010
40. Ding Y, You Z, Jalali S. The composite effect of steel fibres and stirrups on the shear behaviour of beams using self-consolidating concrete. Eng Struct. 2011;33:107–17. https://doi.org/10.1016/j.engstruct.2010.09.023
41. Abbas YM, Fares G, Iqbal Khan M. Depth-dependent flexural behavior of plain and bar-reinforced ultra-high-performance hybrid fiber-reinforced concrete—analytical, numerical, and uncertainty modeling. Structure. 2023;52:723–41. https://doi.org/10.1016/j.istruc.2023.03.184
42. Ergen F, Katlav M. Machine and deep learning-based prediction of flexural moment capacity of ultra-high performance concrete beams with/out steel fiber. Asian J Civ Eng. 2024;25:4541–62. https://doi.org/10.1007/s42107-024-01064-2
43. Zhang Y, Zhu Y, Qiu J, Hou C, Huang J. Impact of reinforcing ratio and fiber volume on flexural hardening behavior of steel reinforced UHPC beams. Eng Struct. 2023;285:116067. https://doi.org/10.1016/j.engstruct.2023.116067
44. Mahmod M, Hanoon AN, Abed HJ. Flexural behavior of self-compacting concrete beams strengthened with steel fiber reinforcement. J Build Eng. 2018;16:228–37. https://doi.org/10.1016/j.jobe.2018.01.006
45. Safhi AEM, Rivard P, Yahia A, Benzerzour M, Khayat KH. Valorization of dredged sediments in self-consolidating concrete: fresh, hardened, and microstructural properties. J Clean Prod. 2020;263:121472. https://doi.org/10.1016/j.jclepro.2020.121472
46. Nematollahzade M, Tajadini A, Afshoon I, Aslani F. Influence of different curing conditions and water to cement ratio on properties of self-compacting concretes. Construct Build Mater. 2020;237:117570. https://doi.org/10.1016/j.conbuildmat.2019.117570
47. Nasr MS, Salman AJ, Ghayyib RJ, Shubbar A, Al-Mamoori S, Al-khafaji Z, et al. Effect of clay brick waste powder on the fresh and hardened properties of self-compacting concrete: state-of-the-art and life cycle assessment. Energies. 2023;16(12):4587. https://doi.org/10.3390/en16124587
48. Nuruzzaman M, Ahmad T, Sarker PK, Shaikh FUA. Rheological behaviour, hydration, and microstructure of self-compacting concrete incorporating ground ferronickel slag as partial cement replacement. J Build Eng. 2023;68:106127. https://doi.org/10.1016/j.jobe.2023.106127
49. Guo Z, Jiang T, Zhang J, Kong X, Chen C, Lehman DE. Mechanical and durability properties of sustainable self-compacting concrete with recycled concrete aggregate and fly ash, slag and silica fume. Construct Build Mater. 2020;231:117115. https://doi.org/10.1016/j.conbuildmat.2019.117115
50. Sharma R, Khan RA. Sustainable use of copper slag in self compacting concrete containing supplementary cementitious materials. J Clean Prod. 2017;151:179–92. https://doi.org/10.1016/j.jclepro.2017.03.031
51. Baloch WL, Siad H, Lachemi M, Sahmaran M. The role of supplementary cementitious materials and fiber reinforcements in enhancing the sulfate attack resistance of SCC/ECC composite systems. Construct Build Mater. 2024;423:135821. https://doi.org/10.1016/j.conbuildmat.2024.135821
52. Casagrande CA, Roque JS, Jochem LF, Correa JN, Medeiros A. Copper slag in cementitious composites: a systematic review. J Build Eng. 2023;78:107725. https://doi.org/10.1016/j.jobe.2023.107725
53. Afshoon I, Sharifi Y. Utilization of micro copper slag in SCC subjected to high temperature. J Build Eng. 2020;29:101128. https://doi.org/10.1016/j.jobe.2019.101128
54. International Copper Study Group. The world copper factbook 2016; 2016. https://icsg.org/
55. Gorai B, Jana RK, Premchand. Characteristics and utilisation of copper slag - a review. Resour Conserv Recycl. 2003;39:299–313. https://doi.org/10.1016/S0921-3449(02)00171-4
56. Al-Jabri KS, Hisada M, Al-Oraimi SK, Al-Saidy AH. Copper slag as sand replacement for high performance concrete. Cem Concr Compos. 2009;31:483–8. https://doi.org/10.1016/j.cemconcomp.2009.04.007
57. Shi C, Meyer C, Behnood A. Utilization of copper slag in cement and concrete. Resour Conserv Recycl. 2008;52:1115–20. https://doi.org/10.1016/j.resconrec.2008.06.008
58. Thomas J, Thaickavila NN, Abrahamb MP. Copper or ferrous slag as substitutes for fine aggregates in concrete. Adv Concr Constr. 2018;6:545–60. https://doi.org/10.12989/acc.2018.6.5.545
59. Mousavi SR, Bahrpeyma A, Afshoon I, Chakkoshi M. Protecting the environment and natural resources using green roller compacted concrete (RCC) containing fine and coarse recycled copper slag aggregates. Process Saf Environ Prot. 2024;186:664–78. https://doi.org/10.1016/j.psep.2024.04.048
60. Ambily PS, Umarani C, Ravisankar K, Prem PR, Bharatkumar BH, Iyer NR. Studies on ultra high performance concrete incorporating copper slag as fine aggregate. Construct Build Mater. 2015;77:233–40. https://doi.org/10.1016/j.conbuildmat.2014.12.092
61. Rajasekar A, Arunachalam K, Kottaisamy M. Assessment of strength and durability characteristics of copper slag incorporated ultra high strength concrete. J Clean Prod. 2019;208:402–14. https://doi.org/10.1016/j.jclepro.2018.10.118
62. Mirhosseini SR, Fadaee M, Tabatabaei R, Fadaee MJ. Mechanical properties of concrete with Sarcheshmeh mineral complex copper slag as a part of cementitious materials. Construct Build Mater. 2017;134:44–9. https://doi.org/10.1016/j.conbuildmat.2016.12.024
63. Gupta N, Siddique R. Durability characteristics of self-compacting concrete made with copper slag. Construct Build Mater. 2020;247:118580. https://doi.org/10.1016/j.conbuildmat.2020.118580
64. Prem PR, Verma M, Ambily PS. Sustainable cleaner production of concrete with high volume copper slag. J Clean Prod. 2018;193:43–58. https://doi.org/10.1016/j.jclepro.2018.04.245
65. Mithun BM, Narasimhan MC. Performance of alkali activated slag concrete mixes incorporating copper slag as fine

17517648, 0, Downloaded from https://onlinelibrary.wiley.com/doi/10.1002/suco.70090 by Metin Katlav - T C Inonu University , , Wiley Online Library on [10/04/2025]. See the Terms and Conditions (https://onlinelibrary.wiley.com/terms-and-conditions) on Wiley Online Library for rules of use; OA articles are governed by the applicable Creative Commons License

aggregate. J Clean Prod. 2016;112:837–44. https://doi.org/10.1016/j.jclepro.2015.06.026
66. Al-Jabri KS, Hisada M, Al-Saidy AH, Al-Oraimi SK. Performance of high strength concrete made with copper slag as a fine aggregate. Construct Build Mater. 2009;23:2132–40. https://doi.org/10.1016/j.conbuildmat.2008.12.013
67. Samabangi A, Eluru A. Industrial copper waste as a sustainable material in high strength SCC. Clean Eng Technol. 2022;6:100403. https://doi.org/10.1016/j.clet.2022.100403
68. Gupta N, Siddique R. Strength and micro-structural properties of self-compacting concrete incorporating copper slag. Construct Build Mater. 2019;224:894–908. https://doi.org/10.1016/j.conbuildmat.2019.07.105
69. Sharifi Y, Afshoon I, Asad-Abadi S, Aslani F. Environmental protection by using waste copper slag as a coarse aggregate in self-compacting concrete. J Environ Manage. 2020;271:111013. https://doi.org/10.1016/j.jenvman.2020.111013
70. Sharma R, Khan RA. Influence of copper slag and metakaolin on the durability of self compacting concrete. J Clean Prod. 2018;171:1171–86. https://doi.org/10.1016/j.jclepro.2017.10.029
71. Sharma R, Khan RA. Durability assessment of self compacting concrete incorporating copper slag as fine aggregates. Construct Build Mater. 2017;155:617–29. https://doi.org/10.1016/j.conbuildmat.2017.08.074
72. Sharma R, Khan RA. Sulfate resistance of self compacting concrete incorporating copper slag as fine aggregates with mineral admixtures. Construct Build Mater. 2021;287:122985. https://doi.org/10.1016/j.conbuildmat.2021.122985
73. Sharma R, Khan RA. Carbonation resistance of self-compacting concrete incorporating copper slag as fine aggregates. J Mater Civ Eng. 2020;32. https://doi.org/10.1061/(asce)mt.1943-5533.0003200
74. Afshoon I, Miri M, Mousavi SR. Comprehensive experimental and numerical modeling of strength parameters of eco-friendly steel fiber reinforced SCC containing coarse copper slag aggregates. Construct Build Mater. 2023;367:130304. https://doi.org/10.1016/j.conbuildmat.2023.130304
75. Afshoon I, Miri M, Mousavi SR. Evaluating the flexural behavior of green copper slag-contained steel fiber reinforced SCC beams with/without initial notches. Construct Build Mater. 2023;395:132316. https://doi.org/10.1016/j.conbuildmat.2023.132316
76. Katlav M, Donmez I, Turk K. Electrical resistivity of eco-friendly hybrid fiber-reinforced SCC: effect of ground granulated blast furnace slag and copper slag content as well as hooked-end fiber length. Construct Build Mater. 2024;438:137235. https://doi.org/10.1016/j.conbuildmat.2024.137235
77. EFNARC. The European Guidelines for Self-Compacting Concrete, Eur. Guidel. Self Compact. Concr. 2005.
78. EFNARC. Specification and Guidelines for Self-Compacting Concrete, Rep. from EFNARC 44. 2002.
79. British Standard Institution. Bs En 12390-3:2019, Test. Hardened Concr. Compressive Strength Test Specimens (2019).
80. ASTM International. C496/C496M—17: Standard Test Method for Splitting Tensile Strength of cylindrical concrete specimens, Annu. B. ASTM Stand. 2017.
81. ASTM C469/C469M–14l. Standard test method for static modulus of elasticity and Poisson's ratio of concrete in compression, Annu. B. ASTM stand; ASTM; 2014. doi:10.1520/C0469_C0469M-14
82. Han B, Ding S, Yu X. Intrinsic self-sensing concrete and structures: a review. Meas J Int Meas Confed. 2015;59:110–28. https://doi.org/10.1016/j.measurement.2014.09.048
83. Sassani A, Ceylan H, Kim S, Gopalakrishnan K, Arabzadeh A, Taylor PC. Influence of mix design variables on engineering properties of carbon fiber-modified electrically conductive concrete. Construct Build Mater. 2017;152:168–81. https://doi.org/10.1016/j.conbuildmat.2017.06.172
84. El-Dieb AS, El-Ghareeb MA, Abdel-Rahman MAH, Nasr ESA. Multifunctional electrically conductive concrete using different fillers. J Build Eng. 2018;15:61–9. https://doi.org/10.1016/j.jobe.2017.10.012
85. Rahman ML, Malakooti A, Ceylan H, Kim S, Taylor PC. A review of electrically conductive concrete heated pavement system technology: from the laboratory to the full-scale implementation. Construct Build Mater. 2022;329:127139. https://doi.org/10.1016/j.conbuildmat.2022.127139
86. ASTM C1611/C1611M-18. Standard test method for slump flow of self-consolidating concrete. ASTM Int, i 2018.
87. Lye CQ, Koh SK, Mangabhai R, Dhir RK. Use of copper slag and washed copper slag as sand in concrete: a state-of-the-art review. Mag Concr Res. 2015;67(12):665–79. https://doi.org/10.1680/macr.14.00214
88. ACI 363R-10. Report on High-Strength Concrete, ACI J. Proc. 2010.
89. Wang R, Shi Q, Li Y, Cao Z, Si Z. A critical review on the use of copper slag (CS) as a substitute constituent in concrete. Construct Build Mater. 2021;292:123371. https://doi.org/10.1016/j.conbuildmat.2021.123371
90. Wu W, Zhang W, Ma G. Mechanical properties of copper slag reinforced concrete under dynamic compression. Construct Build Mater. 2010;24:910–7. https://doi.org/10.1016/j.conbuildmat.2009.12.001
91. Khanzadi M, Behnood A. Mechanical properties of high-strength concrete incorporating copper slag as coarse aggregate. Construct Build Mater. 2009;23:2183–8. https://doi.org/10.1016/j.conbuildmat.2008.12.005
92. de Schepper M, Verlé P, Van Driessche I, de Belie N. Use of secondary slags in completely recyclable concrete. J Mater Civ Eng. 2015;27. https://doi.org/10.1061/(asce)mt.1943-5533.0001133
93. Peirovi M, Labafzadeh MS, Dehghani A, Meftahi F. Durability and mechanical properties of precast concrete curb containing waste copper slag. Mag Concr Res. 2019;71:567–76. https://doi.org/10.1680/jmacr.17.00264
94. Elangovan R, Venkatesh Babu DL, Venkatasubramani R. Studies on high strength self-compacting concrete with copper slag. Int J Appl Eng Res. 2015;10:26879–96.
95. Krishna Chaitanya B, Sivakumar I. Influence of waste copper slag on flexural strength properties of self compacting concrete. Mater Today Proc. 2020;42:671–6. https://doi.org/10.1016/j.matpr.2020.11.059
96. Ameri F, de Brito J, Madhkhan M, Taheri RA. Steel fibre-reinforced high-strength concrete incorporating copper slag: mechanical, gamma-ray shielding, impact resistance, and microstructural characteristics. J Build Eng. 2020;29:101118. https://doi.org/10.1016/j.jobe.2019.101118
97. Damineli BL, Kemeid FM, Aguiar PS, John VM. Measuring the eco-efficiency of cement use. Cem Concr Compos. 2010;32:555–62. https://doi.org/10.1016/j.cemconcomp.2010.07.009
98. Siddique R, Singh M, Jain M. Recycling copper slag in steel fibre concrete for sustainable construction. J Clean Prod. 2020;271:122559. https://doi.org/10.1016/j.jclepro.2020.122559
99. Katlav M, Ergen F. Improved forecasting of the compressive strength of ultra-high-performance concrete (UHPC) via the

17517648, 0, Downloaded from https://onlinelibrary.wiley.com/doi/10.1002/suco.70090 by Metin Katlav - T C Inonu University , , Wiley Online Library on [10/04/2025]. See the Terms and Conditions (https://onlinelibrary.wiley.com/terms-and-conditions) on Wiley Online Library for rules of use; OA articles are governed by the applicable Creative Commons License

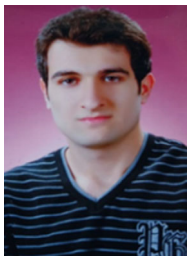
CatBoost model optimized with different algorithms. Struct Concr. 2024;26(1):212–35. https://doi.org/10.1002/suco.202400163

100. Ergen F, Katlav M. Estimation of the shear strength of UHPC beams via interpretable deep learning models: comparison of different optimization techniques. Mater Today Commun. 2024;40:109394. https://doi.org/10.1016/j.mtcomm.2024.109394
101. Tabar ME, Katlav M, Turk K. Explainable ensemble algorithms with grey wolf optimization for estimation of the tensile performance of polyethylene fiber-reinforced engineered cementitious composite. Mater Today Commun. 2025;44:112028. https://doi.org/10.1016/j.mtcomm.2025.112028
102. Katlav M, Tabar ME, Turk K. AI-guided design framework for bond behavior of steel-concrete in steel reinforced concrete composites: from dataset cleaning to feature engineering. Mater Today Commun. 2025;42:111286. https://doi.org/10.1016/j.mtcomm.2024.111286
103. ACI Committee 318. Building Code Requirements for Structural Concrete (ACI 318–19). 2019.
104. Turk K, Cicek N, Katlav M, Turgut P. Electrical resistance of hybrid steel fiber-reinforced self-compacting concrete. J Eng Sci Des. 2022;10:482–94 [in Turkish]. https://doi.org/10.21923/jesd.960538
105. Ren Z, Sun J, Zeng X, Chen X, Wang Y, Tang W, et al. Research on the electrical conductivity and mechanical properties of copper slag multiphase nano-modified electrically conductive cementitious composite. Construct Build Mater. 2022;339:127650. https://doi.org/10.1016/j.conbuildmat.2022.127650
106. Turk K, Cicek N, Katlav M, Donmez I, Turgut P. Electrical conductivity and heating performance of hybrid steel fiber-reinforced SCC: the role of high-volume fiber and micro fiber length. J Build Eng. 2023;76:107392. https://doi.org/10.1016/j.jobe.2023.107392
107. Fiala L, Toman J, Vodička J, Ráček V. Experimental study on electrical properties of steel-fibre reinforced concrete. Proc Eng. 2016;151:241–8. https://doi.org/10.1016/j.proeng.2016.07.362

AUTHOR BIOGRAPHIES



Metin Katlav, Bitlis Eren University, Vocational School of Technical Sciences, Bitlis, Türkiye. Email: mkatlav@beu.edu.tr.



Izzeddin Donmez, Adıyaman University, Vocational School of Technical Sciences, Adıyaman, Türkiye. Email: idonmez@adiyaman.edu.tr.



Asim Kaygusuz, Inonu University, Department of Electrical and Electronics Engineering, Faculty of Engineering, Malatya, Türkiye. Email: asim.kaygusuz@inonu.edu.tr.



Paki Turgut, Inonu University, Department of Civil Engineering, Faculty of Engineering, Malatya, Türkiye. Email: paki.turgut@inonu.edu.tr.



Kazim Turk, Department of Civil Engineering, Faculty of Engineering, Inonu University, Malatya, Türkiye. Email: kazim.turk@inonu.edu.tr.

How to cite this article: Katlav M, Donmez I, Kaygusuz A, Turgut P, Turk K. The workability, mechanical, and electrical properties of steel fiber-reinforced SCC incorporating ultra-fine copper slag as fine aggregate. Structural Concrete. 2025. https://doi.org/10.1002/suco.70090

17517648, 0, Downloaded from https://onlinelibrary.wiley.com/doi/10.1002/suco.70090 by Metin Katlav - T C Inonu University , , Wiley Online Library on [10/04/2025]. See the Terms and Conditions (https://onlinelibrary.wiley.com/terms-and-conditions) on Wiley Online Library for rules of use; OA articles are governed by the applicable Creative Commons License